

Appendix 8.D. CE-QUAL-ICM Setup, Calibration and Withdrawal Scenario Results

John C. Hendrickson, SJRWMD

Acknowledgements

Peter Sucsy¹

Kijin Park¹

Victor Bierman²

Amanda Flynn²

Scott Hinz²

¹St. Johns River Water Management District

²Limno-Tech, Inc. of North Carolina

St. Johns River Water Management District

Palatka, Florida

2011

I. Model Description

CE-QUAL-ICM is a process-based water-quality model designed for the study of eutrophication in fresh and marine aquatic ecosystems (Cercio and Cole, 1993). The model uses an iterative time step solution scheme operating through a finite-difference grid representation of the morphology of the water body, to produce a continuous stream of fixed-time interval predictions for 31 variables (Table 1). Hydrodynamic characteristics of water volume flux are established by a separate model, which in this application is the Environmental Fluid Dynamics Code (Hamrick, 1992). The original application of CE-QUAL-ICM to the Lower St. Johns River (LSJR) was undertaken to facilitate the understanding of eutrophication processes, and to evaluate external nutrient load scenarios that would achieve target values for chlorophyll-*a* and dissolved oxygen on which to base Federal Clean Water Act Total Maximum Daily Loads (Sucusy and Hendrickson, 2004). The U.S. Army Corps of Engineers Engineer Research Development Center performed the initial set-up and calibration of the LSJR application (Tillman et al, 2004), with the sediment diagenesis sub-model (DiToro and Fitzpatrick, 1993) set-up and parameterization performed by the environmental engineering firm Limno-Tech (2005). After this initial set-up, SJRWMD staff assumed stewardship of the model. For the WSIS application, the model domain has been expanded 37 miles upstream through Lake George, to the normal head of tide at the USGS river monitoring station at Astor, and the simulation time interval expanded through 2005. The setup and initial calibration for the expanded temporal coverage was performed by Limno-Tech, Inc. Because the model domain now extends to the head of the estuary, it is hereafter referred to as the St. Johns River Estuary model (SJREM). As the focus for the WSIS modeling is the assessment of the effect of water withdrawals on the magnitude of cyanobacteria-dominated blooms in the freshwater SJRE, results downstream of Racy Pt. (RM 64) are not utilized for this application.

CE-QUAL-ICM is built on mechanistic relationships between underwater irradiance, primary production, carbon and nutrient assimilation, grazing, decomposition and settling. The model minimizes the use of empirical approaches that bypass phytoplankton dynamics in order to simulate aggregate water quality metrics. It is unique among water quality process models in that it is carbon mass-conserving, with the flux of carbon, nitrogen and phosphorus into, and out of, the phytoplankton organic carbon compartment determined by generally recognized assimilation rates and stoichiometric ratios. Phytoplankton growth is governed by temperature and the exposure of the phytoplankton, subject to mixing into and out of the photic zone by the model hydrodynamics, to photosynthetically-active radiation (PAR). Light attenuation is determined by the model of Gallegos (2005) based on chlorophyll-*a*, total suspended solids, and color (represented in the model by refractory dissolved organic carbon). Eutrophication-related water quality metrics, such light attenuation, dissolved oxygen, or chlorophyll-*a*, are governed by the standing stock of the phytoplankton organic carbon pool. The oxygen budget is driven by photosynthesis, respiration, decomposition, and nitrification, in the water column and sediments, and by water surface atmospheric diffusion. Unique capabilities of CE-QUAL-ICM that make it particularly well-suited for the simulation of eutrophication in the SJRE are the inclusion of three phytoplankton groups, to better account for the competitive interactions between groups and across the salinity gradient, and the separation of labile and refractory organic C, N and P pools, to account for the high natural background pool of the largely refractory colored dissolved

organic matter (CDOM). Detailed descriptions of the mathematical formulations that drive model processes can be found in Tillman et al. (2004), and Sucsy and Hendrickson (2004).

Table 1. CE-QUAL-ICM state variables employed in the St. Johns River Estuary application.

CE-QUAL-ICM Variables	
Temperature (°C)	Phosphorus Forms, (as mg L⁻¹ P)
Salinity (ppt)	Orthophosphate
Carbon Forms, (as mg L⁻¹ C)	Labile Dissolved Organic Phosphorus
Cyanobacteria	Refractory Dissolved Organic Phosphorus
Freshwater Diatoms	Labile Particulate Organic Phosphorus
Marine Diatoms	Refractory Particulate Organic Phosphorus
Labile Dissolved Organic Carbon	Particulate Inorganic Phosphorus
Refractory Dissolved Organic Carbon	Cyanobacteria Phosphorus
Labile Particulate Organic Carbon	Freshwater Diatom Phosphorus
Refractory Particulate Organic Carbon	Marine Diatom Phosphorus
Nitrogen Forms, (as mg L⁻¹ N)	Inorganic Suspended Solids (mg L ⁻¹)
Ammonium	Total Suspended Solids (mg L ⁻¹)
Nitrite+Nitrate	Dissolved Oxygen (mg L ⁻¹)
Labile Dissolved Organic Nitrogen	Particulate Silica (mg L ⁻¹)
Refractory Dissolved Organic Nitrogen	Dissolved Silica (mg L ⁻¹)
Labile Particulate Organic Nitrogen	State Variables not Used
Refractory Particulate Organic Nitrogen	Particulate Inorganic Phosphorus
	Chemical Oxygen Demand

Figure 1 depicts the general process flow diagram for CE-QUAL-ICM. C, N and P are apportioned into the phytoplankton at rates specific to the three functional group designations, external nutrient supply and physical, chemical and hydrodynamic setting. In the SJRE application, C, N and P leave the phytoplankton according to group-specific terms for grazing and settling, and enter sequential pools of particulate and dissolved labile forms, which drive general heterotrophic respiration, exerting an effect on the oxygen budget. The three functional phytoplankton groups used in the WSIS application are set up to generally mimic cyanobacteria, freshwater diatoms, and marine diatoms. Freshwater forms have a salinity toxicity, while marine diatoms have a freshwater toxicity.

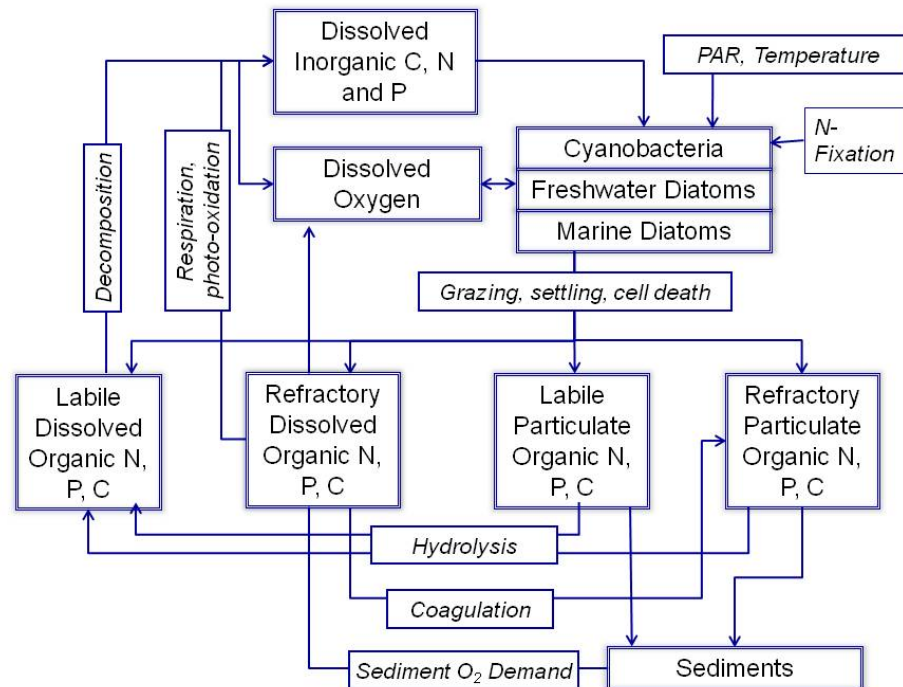


Figure 1. Generalized Process Diagram for CE-QUAL-ICM. For the WSIS application, the three algal groups available in this model version were parameterized to represent cyanobacteria, freshwater diatoms, and marine diatoms. N-fixation is enabled for cyanobacteria. Chlorophyte algae, which typically compose less than ten percent of the phytoplankton biovolume, were combined with the freshwater diatom group for this application.

After heterotrophic decomposition, C leaves the organic pool (inorganic C is not tracked in the model, and is not considered to be limiting), and N and P re-enter the inorganic or refractory pools. In the SJRE adaptation, N can enter the cyanobacteria organic N pool through N-fixation when external N is limiting.

II. Model Set-Up and Parameterization

Model Inputs

The model domain for the SJREM encompasses the tidal freshwater and marine portions of the St. Johns River estuary, a distance of 127 miles (204 km) from above the inlet of Lake George to the Atlantic inner shelf, and includes the major off-line lakes Crescent Lake and Doctor's Lake (Figure 2). The SJREM was set up with ten years of input boundary concentrations, developed to match the 1996 – 2005 time-period of EFDC-simulated hydrodynamic record. A range of river discharge conditions occurred during this simulation window representative of the 50-year record from 1950 through 2009 (Figure 3). For calibration simulations, hydrologic inputs were supplied by observed data wherever available, and simulated data were used for the remaining runoff areas. For scenario simulations, water volume inputs were constructed from hydrologic simulations representative of the respective withdrawal condition.

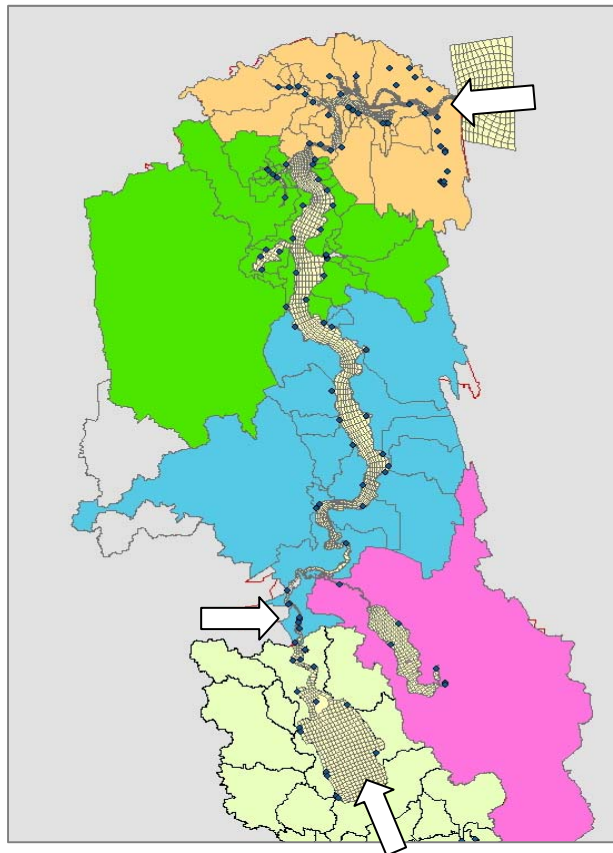


Figure 2. CE-QUAL-ICM domain for the St. Johns River Estuary application. Blue dots identify entry points for predicted input loads, and white arrows identify major boundaries developed with observed data. Contributing basins color-coded to river reach: Yellow = Lake George; Pink = Crescent Lake; Blue – the LSJR Freshwater Reach; Green = LSJR Oligohaline Reach; Tan = LSJR Meso-Polyhaline Reach.

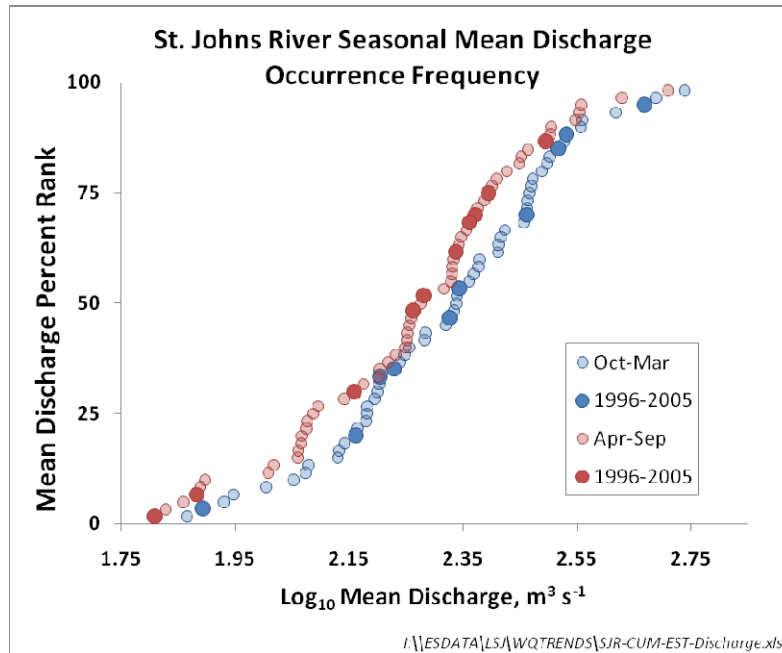


Figure 3. Distribution of CE-QUAL-ICM simulated years within the 50-year St. Johns River discharge record from 1950 – 2009.

Major inputs were entered into the SJRE model domain upstream of Lake George at FL Hwy. 40 (St. Johns River at Astor), at the Ocklawaha River (mid-way between Lake George and the Lower St. Johns), and at the Atlantic inner shelf east of the river mouth (white arrows, Figure 2). The chemical concentration time series inputs for the SJR at Astor, the Ocklawaha mouth, and the Atlantic Ocean were created from measured ambient monitoring data, converted to daily values by linear interpolation. Sampling intervals changed over the simulation record, affecting the precision of the input data stream. For the SJR at Astor, sampling was approximately once every two months through fall of 1998, twice per month for fall of 1998 through fall of 1999, monthly from fall of 1999 through fall of 2004, and then twice per month for the remainder of the record (Figure 4a). The Ocklawaha mouth was sampled quarterly in 1996, monthly in 1997, and twice per month from 1998 through the remainder of the record (Figure 4b). For the Atlantic Ocean boundary, inner shelf chemistry collection was so infrequent that all data were combined to make an annual repeating time series as a function of Julian day. Though this data series does not capture the temporal variability over the 10-year simulation, it has no effect on the results of the SJRE freshwater reach.

Because discharge controls a number of properties and chemical concentrations that in turn control phytoplankton production and standing stock, the discharges on chemistry sampling dates were compared to the full 1996 – 2005 discharge occurrence frequency to visually assess potential bias. An overlay of sample date discharges on the full record indicates that the samples appear to be well distributed over the discharge record (Figure 5).

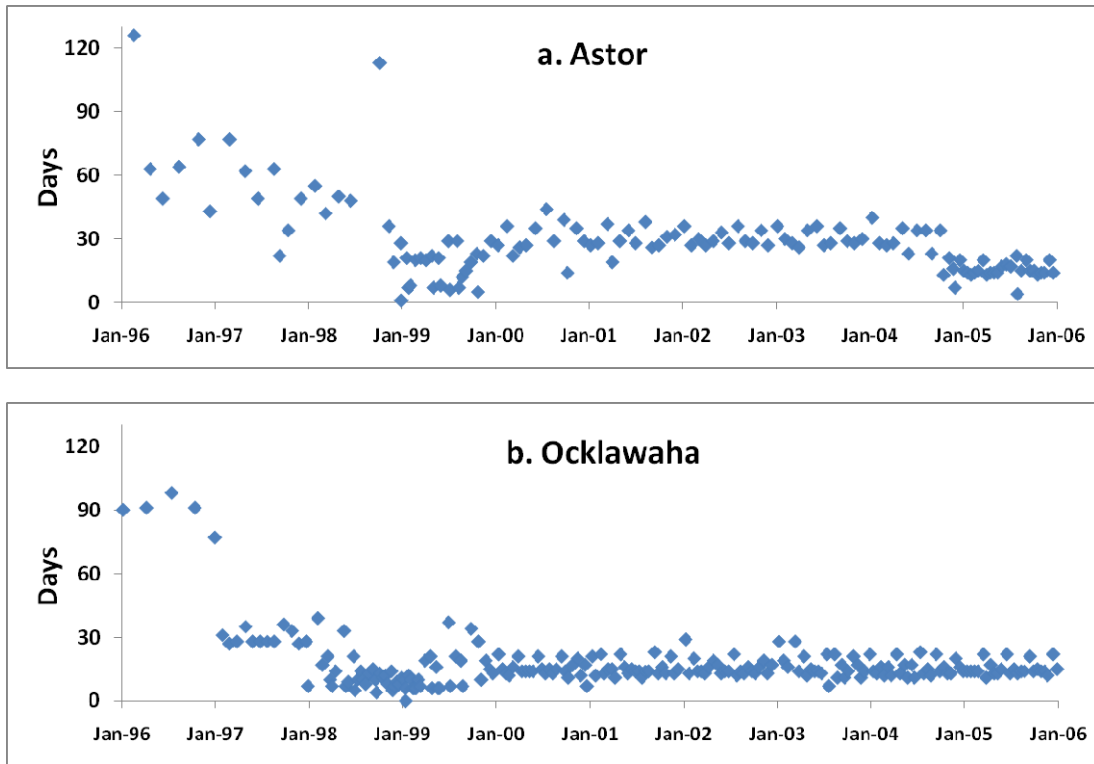


Figure 4. Days since previous sampling date for (a) the Middle St. Johns River at FL State Road 40 (Astor) and (b) the Ocklawaha River mouth.

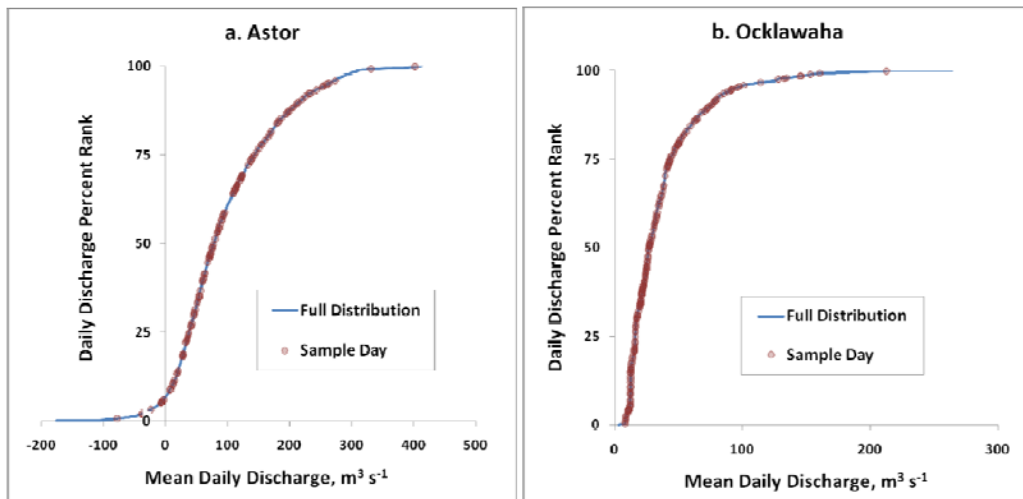


Figure 5. Sampling date occurrence in relation to the discharge frequency distribution for (a) the Middle St. Johns River at FL State Road 40 (Astor) and (b) the Ocklawaha River mouth.

Loads from point sources and tributaries to the model domain other than the upstream SJR and Ocklawaha were set to the conditions that existed from 1995 – 1999. This time interval was selected because it matched that used for the lower St. Johns River Total Maximum Daily Load computations, and because it was consistent with the 1995 land use that was used for the WSIS base case. Point source concentrations were set to the mean value obtained from discharge monitoring reports. Thirty-three major point sources discharge to the main stem of the SJRE, with mean daily discharge ranging from 0.4 to 35 million gallons per day. Most of these point sources are downstream of the freshwater reach and outside of the area of interest for the WSIS simulations, though the largest single point source discharge, a pulp mill, is in the freshwater reach just downstream of Palatka. Point sources supply on average 6 and 22 percent of the anthropogenic N and P to the freshwater reach between Palatka and Racy Pt. There are no point source discharges between Palatka and Astor. Because point sources supply a relatively constant background load, the freshwater reach P concentration shows less of a tendency to decrease during low flow than does Lake George. In the early 2000's, the two largest point sources in the freshwater LSJR began to institute a number of process improvements, and as a result the 1995-99 mean point source load overestimates the actual point source contribution towards the end of the 1996 – 2005 simulation time period.

There are 110 tributary inflow points in the SJREM domain. Because few of these have regular monitoring data, their concentrations were predicted by a nonpoint source runoff model referred to as the Pollution Load Screening Model (Adamus and Bergman, 1993). This model employs land use-characteristic chemical concentrations that were determined through a multi-watershed multiple regression approach that objectively assigns constituent concentrations to land uses (Hendrickson and Konwinski, 1998). Assigning watershed runoff concentrations by this method implicitly incorporates stream attenuation and provides a concentration that is representative of that delivered to the receiving water. The model has three sets of constituent concentrations that conform to the seasonal (Dec-Mar, Apr-Jul, and Aug-Nov) pattern in tributary N, P and C that is evident in NE Florida, arising from the general trend in terrestrial plant productivity, agronomic seasons, and soil flooding and redox-mediated constituent mobility.

The 1995 land use was used for the entire 10-year watershed model tributary concentration prediction. Runoff volume was simulated with the HSPF watershed model and was the same used for WSIS hydrologic predictions. Watershed load was calculated as the product of the two, and is time varying in the sense that water volumes match the precipitation patterns over the simulation pattern, but is fixed in the sense that concentration reflected the 1995 land use. Direct atmospheric wet and dry deposition was determined from NADP ground stations as per the methods described in Pollman and Roy (2003). The method for compartmentalization of C, N and P into labile and refractory forms is described in Hendrickson et al. (2007).

To construct the withdrawal scenario input data stream for the SJREM, the boundary, tributary, and point source loads were retained from the calibration, but were conveyed into the model domain with the water volumes of the respective scenario. This results in small changes in constituent concentrations for withdrawal scenarios, as the load is conveyed with a different water volume. Water withdrawals lead to an increase in concentration at the Ocklawaha and middle St. Johns boundaries, while under the 2030 land use scenarios, runoff volume may be greater, potentially leading to lower concentrations for some tributary inputs.

This approach was selected as a way to isolate the hydrologic effect of water withdrawal, irrespective of nutrient loading, on ecological conditions. Maintenance of current nutrient loading allows simulation results from the SJRE model to be compared with results from empirical models (Chapter 8. Plankton) and is a reasonable assumption given uncertainty in future conditions. Also, this approach approximates the potential that constituents removed with water withdrawal could be returned to the river in reverse-osmosis reject water. In reality, only a fraction of the withdrawn constituents would be returned in the reject water stream, and in the case of phosphorus and colored dissolved organic matter, this fraction would likely be very small (though it is estimated that a large fraction of polar anions, such as Cl and NO₃, would be returned). This approach essentially assumes that all constituents are returned, representing the worst-case change in constituent concentration.

Algal Carbon Conversion Factors

Chlorophyll-*a* is the principal means through which algal standing stock and the ambient condition is assessed in water quality monitoring programs, and is relied on to evaluate, and to express modeling study findings. Because CE-QUAL-ICM simulates algal C, it is necessary to arrive at a reasonable conversion between these two variables to compare model results to observed data, and to present scenario results. A conversion is derived here in a two step analysis, by first establishing the relationship between phytoplankton biovolume and phytoplankton C, and then using this measure of phytoplankton C to propose a model relating phytoplankton C to chlorophyll *a*.

The relationship between algal C and chlorophyll-*a*, and between algal C and N and P for that matter, is not constant, and can vary due to nutrient limitation, temperature, species, light environment, and growth rate (Gosselain et al., 2000; Klausmeier et al. 2004). A ratio of 50:1 algal C to chlorophyll *a* is a commonly accepted rule of thumb, though studies that directly measure the two metrics generally determine ratios in a range from 30 to 60 (Gosselain et al., 2000), with extremes of 10 to 333 reported (Cloern et al., 1995).

Some inferences can be drawn from the nature of the relationship between chlorophyll *a* and seston C, N and P (Figure 6). Because the seston contains particulate organic (and, in the case of P, inorganic) material other than the phytoplankton, the bottom edge of the ordination of points between chlorophyll *a* and particulate C, N and P should represent the condition where non-algal seston is at a minimum, total POC \approx algal POC, and should conform to the theoretical stoichiometric ratios for phytoplankton. For freshwater SJRE data collected at Racy Pt. and Lake George, the standard stoichiometric ratios do appear to conform to the lower limit of data scatter for chlorophyll *a* concentrations below about 40 $\mu\text{g/L}$. Above this concentration, when it would be expected that phytoplankton would begin to dominate the seston, and the data points would begin to converge on the expected characteristic phytoplankton ratios, the departures in fact increase. This increased departure is positive for C and N, indicating that the C:chlorophyll *a* and N:chlorophyll *a* ratios increase at high biomass levels. Conversely, the P departure is negative, indicating that the P:chlorophyll *a* (and also the C:P and N:P) ratio decreases at high biomass levels. This could occur at high biomass levels in nitrogen-fixing cyanobacterial blooms under

increasing levels of P deficiency, or as blooms transition from the exponential to stationary growth phase (Cloern et al., 1995; Klausmeier et al. 2004).

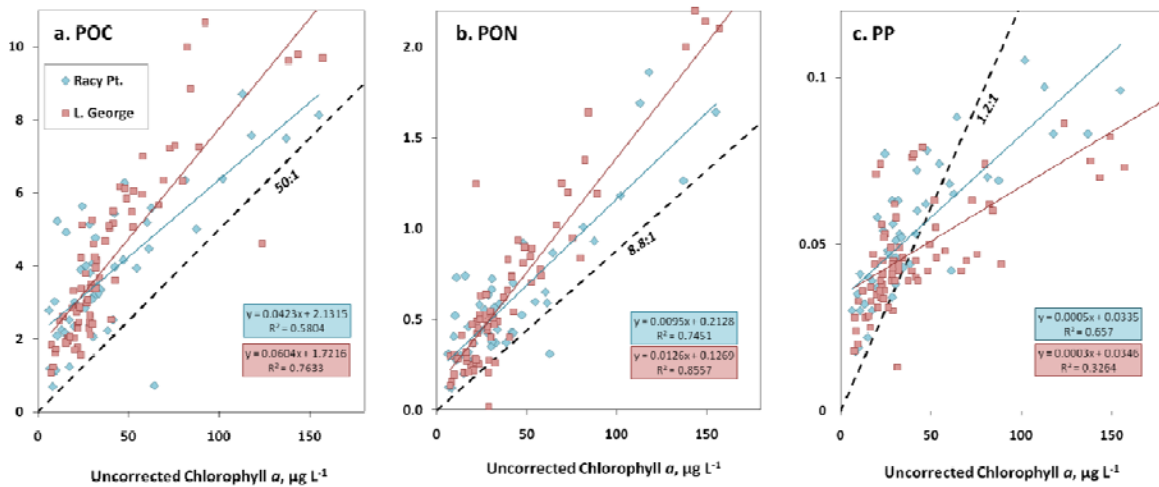


Figure 6. Scatter plots of uncorrected chlorophyll *a* and particulate C, N and P, for the monitoring stations at Lake George and Racy Pt, 1998 – 2004. Black dashed lines represent the generally accepted ratio of 50:1 C:chlorophyll *a*, or the similar ratio converted to N and P using the Redfield C:N and C:P mass ratios.

Algal biovolume, though a relatively imprecise measure, is theoretically directly related to algal C so should therefore be linear as algal biomass increases, irrespective of physiological changes occurring in the phytoplankton. A number of biovolume – carbon relationships have been developed for algae. These models are typically fit to a power function of the form:

$$\text{Algal C} = a * [(\text{Algal cell volume})^b]$$

to account for the changing C:biovolume ratio as cell size changes. In this power function model form, the carbon per cell must first be calculated, and then summed based on cell count per volume. If applied to the total assemblage biovolume, a $b > 1$ will predict a total algal C greater than the sum of the individual cell C, and a $b < 1$ will predict a total algal C that is less than the cell sum. However, Montagnes et al. (1994) noted that for all of the models they tested, none produced a b that was significantly different from 1, and in most of the models reviewed, values for b are very close to 1. Hence, in many applications, direct single-factor conversions have been commonly used (Hessen et al., 2003; Jahnke and Mahlmann, 2009; Reynolds, 1984; Rocha and Duncan, 1985). Single-factor conversions also have the advantage in that they do not require computations for each cell size in the assemblage.

Most of the biovolume to phytoplankton C functions have been developed for marine phytoplankton. Overall, marine biovolume models predict algal organic carbon lower than that observed for the freshwater SJRE, perhaps due to the predominance of diatoms in these marine assemblages. Diatom biovolumes include the silica frustules of varying size, may include gas

vacuoles, and are often larger than freshwater diatoms, resulting in reduced carbon per unit biovolume in comparison to freshwater cyanobacteria. Rocha and Duncan (1985) assembled a set of conversions for freshwater phytoplankton based on published results from 41 lab cell cultures representing 27 species of chlorophytes, cyanophytes, and diatoms (the frequently cited earlier work of Chalk (1981) are also included). Rocha and Duncan (1985) proposed the following generalized model for all freshwater phytoplankton:

$$\text{Algal C} = 0.1204 * [(\text{Algal cell volume})^{1.051}]$$

where algal cell C is in pg, and algal cell volume is measured in μm^3 . However, like other investigators, Rocha and Duncan (1985) concluded that b was not significantly different than 1, and that algal carbon could be determined directly from the conversion of “approximately” $2 \text{ pg C} / \mu\text{m}^3$. By iteratively changing values near this conversion, and visually inspecting the match between biovolume to algal C, a conversion of $0.26 \text{ pg C} / \mu\text{m}^3$ algal biovolume was selected for SJRE freshwater phytoplankton. The proximity of this phytoplankton C conversion with respect to the biovolume versus POC scatter plot, and with respect to N and P, is shown in Figure 7.

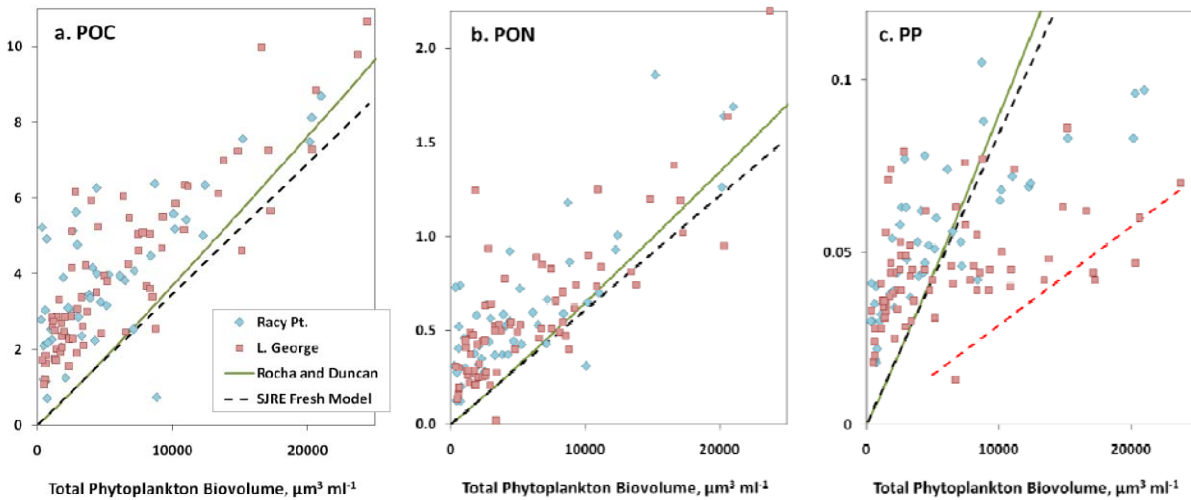


Figure 7. Scatter plots of phytoplankton biovolume and particulate C, N and P, for the monitoring stations at Lake George and Racy Pt, 1998 – 2004, and predicted phytoplankton C by the model of Rocha and Duncan (1985) (solid green line), and the conversion selected for SJRE freshwater phytoplankton (dashed black line). Dashed red line on the PP plot (c) is a translation of the maximum C:P ratio (120) set in CE-QUAL-ICM.

As previously indicated, diatom algae have structural features that theoretically would lead them to have a different biovolume to C relationship (Strathmann, 1967). In the studies compiled by Rocha and Duncan (1985), mean C to volume ratios for diatoms and cyanobacteria were nearly identical (OC:biovolume for diatoms = 0.154 (range = 0.076 – 0.242), and for cyanobacteria = 0.156 (range = 0.032 – 0.277)). To assess possible differences between diatom and cyanobacteria C to biovolume relationships for the freshwater SJRE, the POC and paired biovolume data were divided into cyanobacteria-dominant and diatom-dominant subsets, and the scatter plots compared to the algal C predicted by the SJRE relationship of 0.26 pg C/ μm^3 algal biovolume (Figure 8). The same relationship appears to similarly bound the lower edge of the seston POC for both groups, suggesting that the same conversion is generally applicable to both groups.

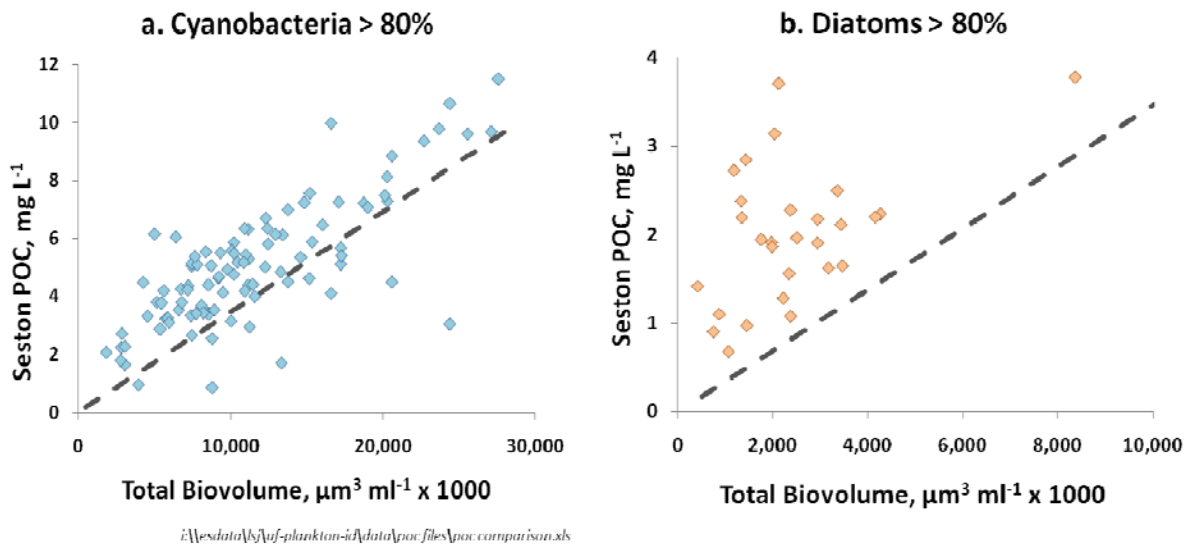


Figure 8. Comparisons of SJRE algal OC predictions to total seston POC for cyanobacterial (a) and diatom (b) dominated sampling events, based on percent of total biovolume. Red line represents the linear 0.26 pg C/ μm^3 algal biovolume conversion. Note the change in axes scale for diatom-dominated events.

Comparison of Algal C to Chlorophyll a

Applying the proposed freshwater SJRE algal carbon conversion of 0.26 pg C/ μm^3 algal biovolume, mean and median algal C:chlorophyll *a* ratios for the combined biovolume and chlorophyll *a* data set were calculated and are listed in Table 2. The mean and median values are within commonly cited ratios for algal C:chlorophyll *a* (for the most part between 27 – 67; Riemann et al. 1989), with the 5th and 95th percentile ratios generally running from 50 to 200 percent of the median.

In their model analysis, Cloern et al. (1995) emphasize two recognized factors driving variation in the phytoplankton carbon:chlorophyll ratio: 1) that C:chlorophyll ratio increases with increasing nutrient stress; and 2) that the rate of change in C:chlorophyll with nutrient stress is dependent upon the light exposure. C:chlorophyll increases linearly with increasing light level (Geider, 1987), a relevant characteristic in the St. Johns, which tends to exhibit higher K_d in fall and winter due to greater inputs of CDOM.

Table 2. Mean and median calculated algal C:Chlorophyll-*a* ratios for the freshwater SJRE.

Location	Mean	Median	5th %ile	95th %ile
Lake George	50	46	19	91
Buffalo Bluff	48	44	21	92
Palatka	39	36	18	75
Racy Pt.	39	39	16	81

These factors combine to create a general pattern in algal C:chlorophyll-*a* in relation to algal biomass that is depicted in Figure 9. Low phytoplankton biomass coincides with periods when water temperature is low, nutrient supply is in excess of growth needs, and river water is darkly stained, resulting in low underwater light levels, conditions that encourage chlorophyll-*a* to be high relative to algal C. When algal biomass is high (chlorophyll *a* > 40 µg/L), nutrient limitation is more common, creating a condition when algal C is likely to be high relative to chlorophyll *a*.

This general pattern was integrated into a simple empirical model to convert CE-QUAL-ICM algal carbon predictions into chlorophyll-*a* of the form:

$$\text{Algal OC:chlorophyll-}a = \text{TANH}(1.5264 * \text{LN}(\text{chlorophyll-}a) - 5.0189) * 16 + 44;$$

To convert observed chlorophyll-*a* to algal carbon, this equation was transformed to:

$$\text{Algal OC:chlorophyll-}a = \text{TANH}(1.19187 * \text{LN}(\text{algal OC}) - 8.4) * 16 + 44;$$

for both chlorophyll-*a* and algal OC in µg C/L.

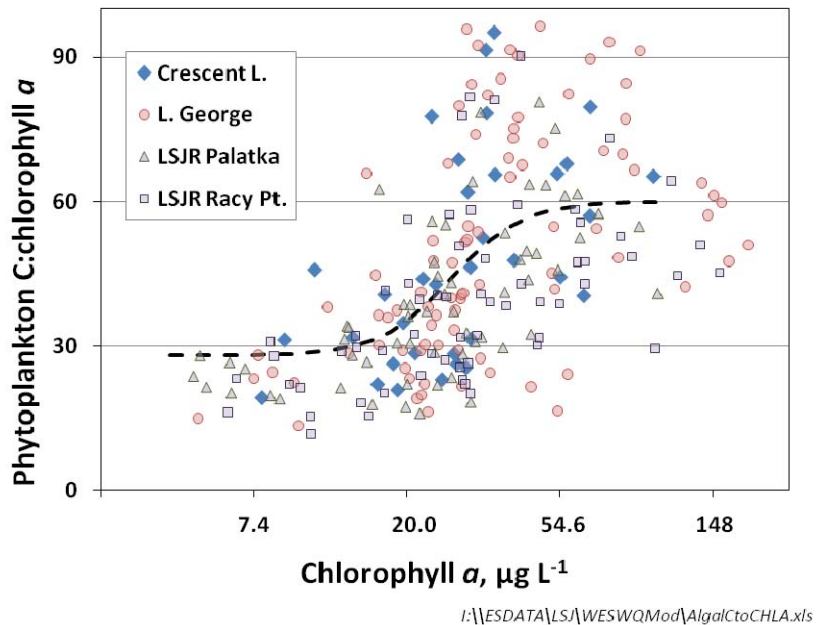


Figure 9. Biovolume-calculated phytoplankton C:Chlorophyll *a* ratio as a function of chlorophyll *a*. Black dashed line is predicted phytoplankton C:chlorophyll *a* based on the hyperbolic tangent function model.

III. Calibration and Scenario Results

Calibration: Background

Surface water quality data from two long-term monitoring locations, the northern 1/3rd of Lake George, and the LSJR at Racy Pt., are relied upon for the model calibration and scenario assessment. In-river sampling frequency for these locations is graphically represented in Figure 10. To condense model simulation results, daily averages were calculated for a group of model cells representative of the location where ambient surface water samples were collected (Figure 11). Results from the top four layers of the six-layer grid were averaged, to approximate the vertical integrated sampling method used in the ambient monitoring programs.

Calibration of the SJREM was undertaken by modifying the algal kinetic control parameters, within bounds defined by the literature and LSJR-specific investigations, to optimize the correspondence between the simulated output with the in-river observed data. Because the base LSJR model had already been applied for the TMDL assimilative capacity analysis, control parameter adjustments were limited and focused primarily on cyanobacteria grazing loss and salinity intolerance, based on LSJR-specific studies (Paerl et al., 2002), and to settling terms to match the net phosphorus loss calculated from the Lake George input – output nutrient budget. The kinetic control parameter set used in the WSIS application is listed in Table 3.

Figure 10. Intervals between sampling events for (a) Lake George and (b) Racy Pt., 1996 – 2005.

Figure 11. Model grid cells averaged to represent the condition at (a) Lake George, and (b) Racy Pt., for the WSIS SJREM simulations. Red circles indicate the locations of ambient water quality monitoring stations combined to represent mean conditions for these sites.



Differences between observed data and model results can arise from 1) the correspondence of the external load used as model input to the actual load; 2) spatial and temporal limits of the observed data used to establish the “true” condition; and 3) model capability, governed by parameterization and algorithm suitability. As previously discussed in the model set-up and parameterization section, the inputs to the SJREM for the WSIS application are developed from a combination of observed and simulated data of varying temporal precision and accuracy. Though the major boundary inputs are developed from 1996 – 2005 time series observed data, point source and tributary loads are derived from long term average or simulated data. Hence this component of the input load deviates slightly from the true condition, due to reductions and re-apportionment of point source loads, and due to changes in agricultural development and urbanized area within the LSJR basin between 1995 and 2005 (Hendrickson and Hart, 2007).

With respect to the observed data used to establish the “true” condition, pulsing flow and nutrient inputs of the fresh SJRE result in seasonal phytoplankton booms with significant spatial and temporal variability, apparent in transect sampling (Figure 12) and occasional sampling efforts performed at high temporal intensity. Blooms in the exponential growth phase can expand and collapse rapidly, making it difficult, when sampling intervals are several weeks to a month or more, to definitively identify the timing and magnitude of bloom peak. Temporal gaps pose less of a limitation for interpreting the condition at Racy Pt., which for most of the simulation time-period was monitored twice per month; however, sampling gaps of 30 days or more are common in the Lake George data record through 2004 (Figure 10).

Table 3. CE-QUAL-ICM kinetics control parameter set used for the SJRE WSIS simulations.

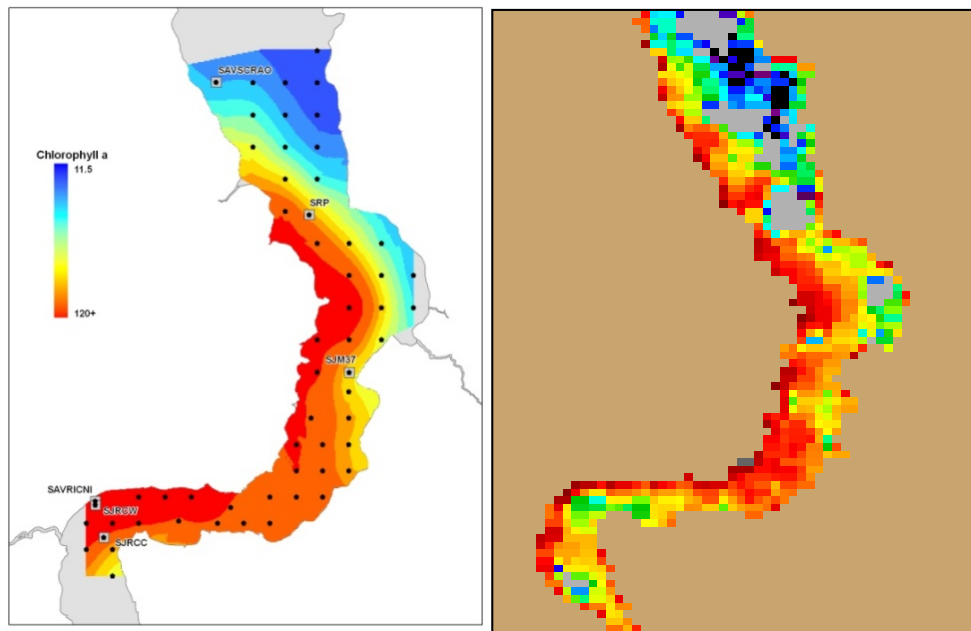
Predation Function	Units	Abbrev.	Value
Reference Temperature for predation	°C	TRPR	20
Predation decay coefficient	°C ⁻¹	KTPR	0.069
Fraction Inorganic N by Predation	Fraction	FNIP	0.3
Fraction Dissolved Labile Organic N by Predation	Fraction	FLNDP	0.25
Fraction Dissolved Refractory Organic N by Predation	Fraction	FNRDP	0.1
Fraction Particulate Labile Organic N by Predation	Fraction	FNLP	0.25
Fraction Particulate Refractory Organic N by Predation	Fraction	FNRP	0.1
Fraction Inorganic P by Predation	Fraction	FPIP	0.5
Fraction Dissolved Labile Organic P by Predation	Fraction	FPLDP	0.38
Fraction Dissolved Refractory Organic P by Predation	Fraction	FPRDP	0.02
Fraction Particulate Labile Organic P by Predation	Fraction	FPLP	0.09
Fraction Particulate Refractory Organic P by Predation	Fraction	FPRP	0.01
Fraction Dissolved Labile Organic C by Predation	Fraction	FCLDP	0.2
Fraction Dissolved Refractory Organic C by Predation	Fraction	FCRDP	0.1
Fraction Particulate Labile Organic C by Predation	Fraction	FCLP	0.6
Fraction Particulate Refractory Organic C by Predation	Fraction	FCRP	0.1
Fraction Diatom Si Available by Predation	Fraction	FSAP	0.3

Appendix 8.D

Phytoplankton Growth Kinetics			Cyanobacteria	Fresh Diatoms	Marine Diatoms
Nitrogen-to-carbon ratio of algae	g N / g C	ANC1	0.175	0.175	0.175
Minimum cell quota	g P / g C	Q01	0.005	0.005	0.005
Si:C Ratio	g Si / g C	ASC1	0	0.4	0.4
Salinity Toxicity Factor	day ⁻¹	STF1	4	0.6	0.5
Half-saturation concentration for N uptake by algae	mg N/L	KHN1	0.015	0.015	0.015
Half-saturation concentration for P uptake by algae	mg P/L	KHP1	0.001	0.001	0.001
Half-saturation concentration for Si uptake by algae	mg Si/L	KHS1	0	0.05	0.05
Half-Saturation Conc. DOC Excretion	mg C/L	KHR1	0.5	0.5	0.5
Half-Saturation Conc. Salinity Toxicity	g/L	KHST1	4	2	5
Half-Saturation Conc. N-Fixation	mg N/L	KHNFIX	0.01	N/A	N/A
Fraction of N-Fixers		FNFIX	0.25	N/A	N/A
Minimum Illumination for Algal Growth	μE m ² s ⁻¹	ALPHMN	10	6	6
Sub-Optimal Illumination Rate		ALPHRAT	0	0	0
Photo-respiration		PRSP1	0.25	0.25	0.25
Maximum Uptake Velocity		VMAX1	0.005	0.005	0.005
Growth Rate Temperature Function		TMP1	27	20	20
Reference Temperature for Metabolism		TR1	20	20	20
Effect of Temperature Below Tm on Algal Growth	°C ⁻²	KTG11	0.05	0.01	0.01
Effect of Temperature above Tm on Algal Growth	°C ⁻²	KTG12	0.0005	0.01	0.01
Effect of Temperature on Algal Basal Metabolism	°C ⁻¹	KTB1	0.0322	0.0322	0.0322
Fraction Inorg. N from Algal Metabolism	Fraction	FNI1	0.35	0.35	0.35
Fraction Labile diss. organic N from Algal Metabolism	Fraction	FNLD1	0.2	0.2	0.2
Fraction Refractory diss. Organic N from Algal Metabolism	Fraction	FNRD1	0.1	0.1	0.1
Fraction Labile Part. Organic N from Algal Metabolism	Fraction	FNLP1	0.25	0.25	0.25
Fraction Refractory Part. Organic N from Algal Metabolism	Fraction	FNRP1	0.1	0.1	0.1
Fraction Diss. Inorganic P from Algal Metabolism	Fraction	FPI1	0.75	0.75	0.75
Fraction Labile Diss. Organic P from Algal Metabolism	Fraction	FPLD1	0.2	0.2	0.2
Fraction Refractory Diss. Organic P from Algal Metabolism	Fraction	FPRD1	0.05	0.05	0.05
Fraction Labile Part. Organic P from Algal Metabolism	Fraction	FPLP1	0	0	0
Fraction Refractory Part. Organic P from Algal Metabolism	Fraction	FPRP1	0	0	0
Fraction Labile Diss. Organic C from Algal Metabolism	Fraction	FCLD1	0	0	0
Fraction Refractory Diss. Organic C from Algal Metabolism	Fraction	FCRD1	0	0	0
Fraction Labile Part. Organic C from Algal Metabolism	Fraction	FCLP1	0	0	0
Fraction Refractory Part. Organic C from Algal Metabolism	Fraction	FCRP1	0	0	0
Maximum Production Rate	day ⁻¹	PMx	200	400	400
Basal Metabolism at Ref. Temp.	day ⁻¹	BMRx	0.05	0.05	0.05
Predation Rate at Ref. Temp.	day ⁻¹	BPRx	0.02	0.1	0.1

The most significant limitation in the capability of CE-QUAL-ICM relates to the model's lack of an algorithm to simulate cyanobacteria bloom crashes. In the freshwater SJRE, cyanobacteria blooms, once expanded to the stationary phase due to full exploitation of available growth resources, frequently crash, i.e., disappear abruptly. These sudden disappearances are accompanied by significant dissolved oxygen depression, indicating rapid bloom senescence and a transfer of algal organic matter to the labile organic carbon pool. The cause of these bloom crashes is at present theoretical. Possible causes include meteorological events that induce sudden destabilization of the water column, or viral predation, enhanced by phosphorus limitation (Brussaard et al., 1995; Bratbak et al, 1993; Wilson et al, 1996 Wilson et al. 1998; Williamson and Paul, 2004; Weinbauer et al., 2000). Incomplete knowledge regarding the triggers for bloom crashes made it difficult to construct a model algorithm to predict this phenomenon, and as a result the model predicts sustained phytoplankton biomass through the favorable spring and summer growth conditions. For this reason, bloom duration statistics were not utilized from the CE-QUAL-ICM simulations.

Figure 12 . Contour map of chlorophyll-*a* concentration (left), and MERIS satellite image (right) of a bloom in the LSJR fresh reach in May 2010. MERIS image reflectance intensities are uncalibrated to St. Johns River phytoplankton density, so the color ramp was set in this image to match the transect data results.



In consideration of the limitations in the model algorithms, the selected input loads, and the available in-river calibration data, model optimization and veracity assessment have been directed toward the ability of the model to replicate the annual and inter-annual patterns in a relative, rather than absolute sense. The model skill assessment is based primarily upon its ability to match the observed data in bloom magnitude in relation to the inter-annual patterns in residence time and growth resource availability, primarily phosphorus.

Calibration: Performance

The time series of simulated and corresponding observed chlorophyll-*a* and TP for Lake George and Racy Pt. are shown in Figures 13 and 14. Matched-date observed minus simulated differences are shown in Figure 15, and annual median differences between observed and simulated chlorophyll-*a* and TP are listed in Table 4. Simulated chlorophyll-*a* for both locations matches the seasonal pattern (Figure 13), though there is a clear tendency in the simulated peak biomass to remain elevated, rather than peak and fall as is apparent in the observed data. Also apparent are a number of years in which simulated maximum chlorophyll-*a* exceeds the observed data, particularly for Racy Pt. The Racy Pt. 1997 over-prediction can be attributed to a titanium mine reservoir levee breach that flooded the river with turbid, opaque water, truncating what was projected to be a large bloom that year. (This event was not incorporated into the model input load.) Over-prediction of spring TP loads may have stimulated model bloom development greater than the observed (model TP ~20 percent greater than observed in 2002 and 2004), while reduced sampling resolution in 2003 and 2004 may have led to missed bloom peaks in the ambient monitoring. The largest differences between observed and simulated chlorophyll-*a* occur at bloom crash nadirs, and during temporal mismatches during the bloom exponential growth phase. In dry years, observed blooms appear to accelerate sooner than simulated, then crash, creating a sharp oscillating positive to negative pattern in the difference time series.

From 1996 through 2005, observed chlorophyll-*a* at both Lake George and Racy Pt. exhibited significant downward trends, while TP is trending upward, driven largely by higher discharge at the end of the record from 2003-05. These long-term trends are also evident in the simulated data for Lake George, though the downward chlorophyll-*a* trend is not significant. Racy Pt. simulation results do not match these trends. Because it is farther from the upstream input boundary, simulated TP at Racy Pt. is more reliant on the “facsimile” external TP load provided as model input, which may be over-predicted at low flow due to reductions that have occurred in actual point source load.

Median Racy Pt. simulated TP is significantly larger than the observed for the dry years from 1999 through 2001 (Table 4). Through the simulation interval, the Lake George observed – simulated TP difference increases (Figure 15), and median TP is significantly greater from 2003-05 (Table 4). There is no trend in Lake George chlorophyll-*a* difference through the simulation. The difference between observed and simulated TP trends upward at Racy Pt., while the difference in chlorophyll-*a* trends down.

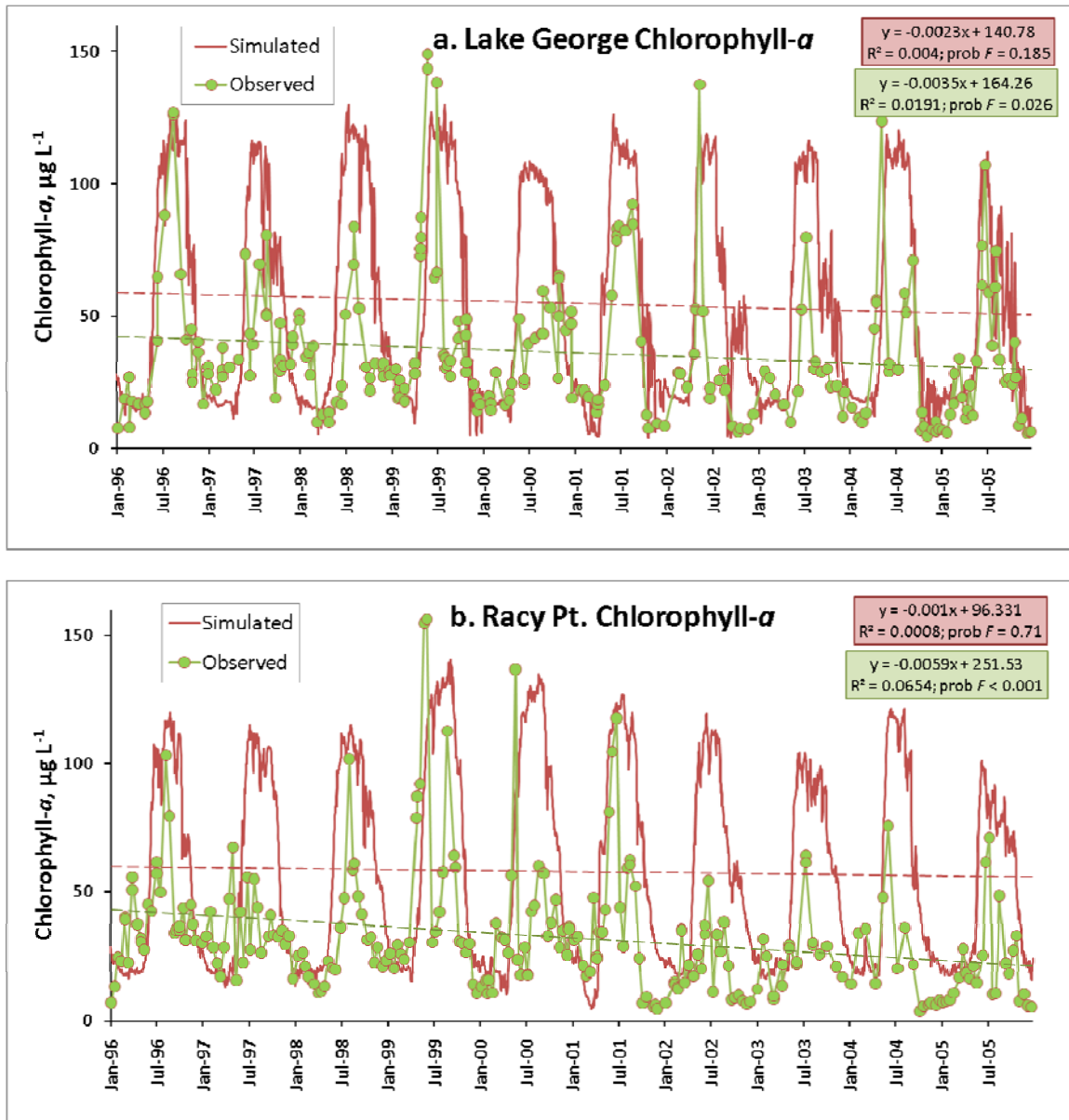


Figure 13. Time series of simulated and observed chlorophyll- a at (a) Lake George and (b) Racy Pt.

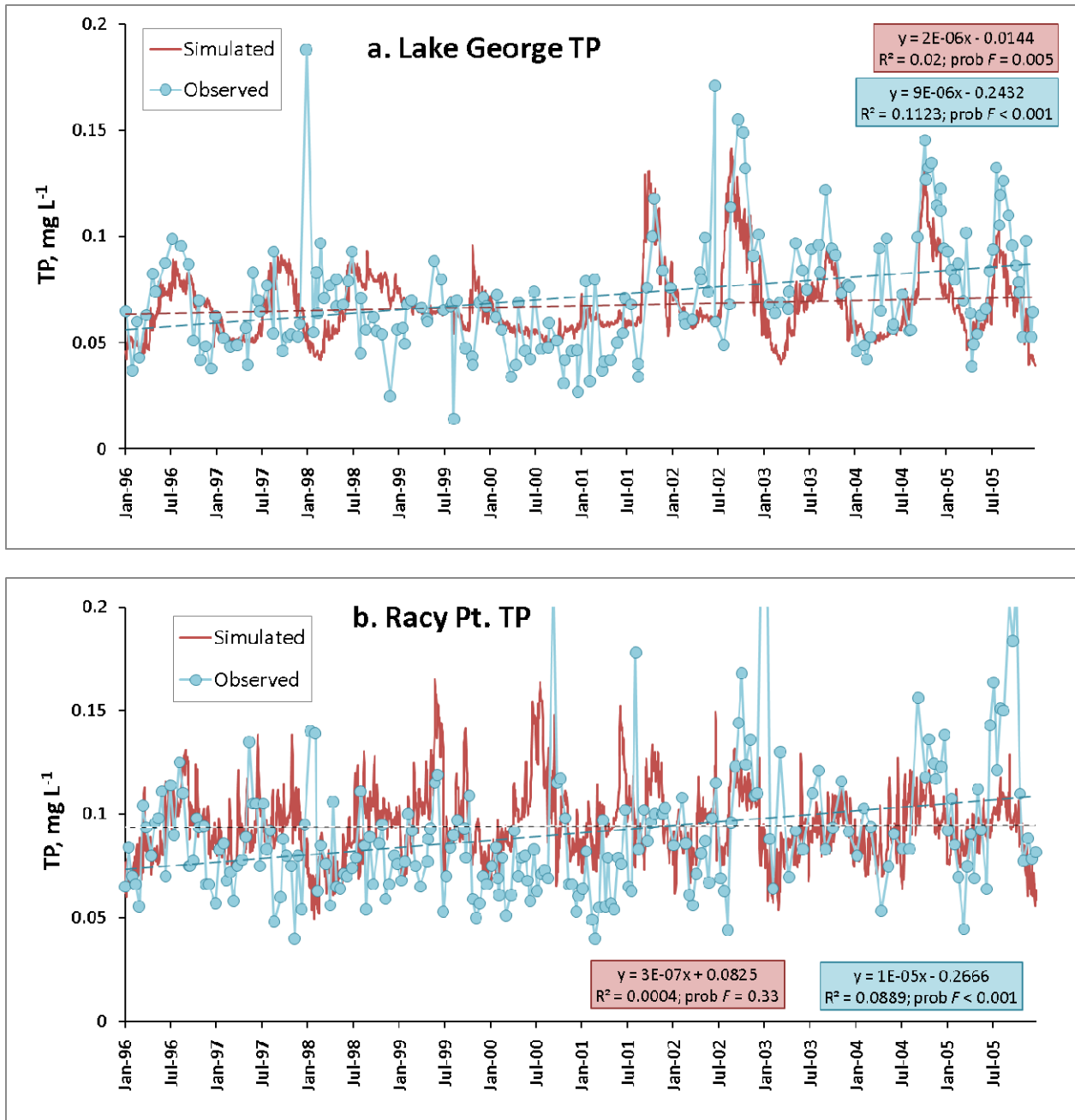


Figure 14. Time series of simulated and observed total phosphorus at (a) Lake George and (b) Racy Pt.

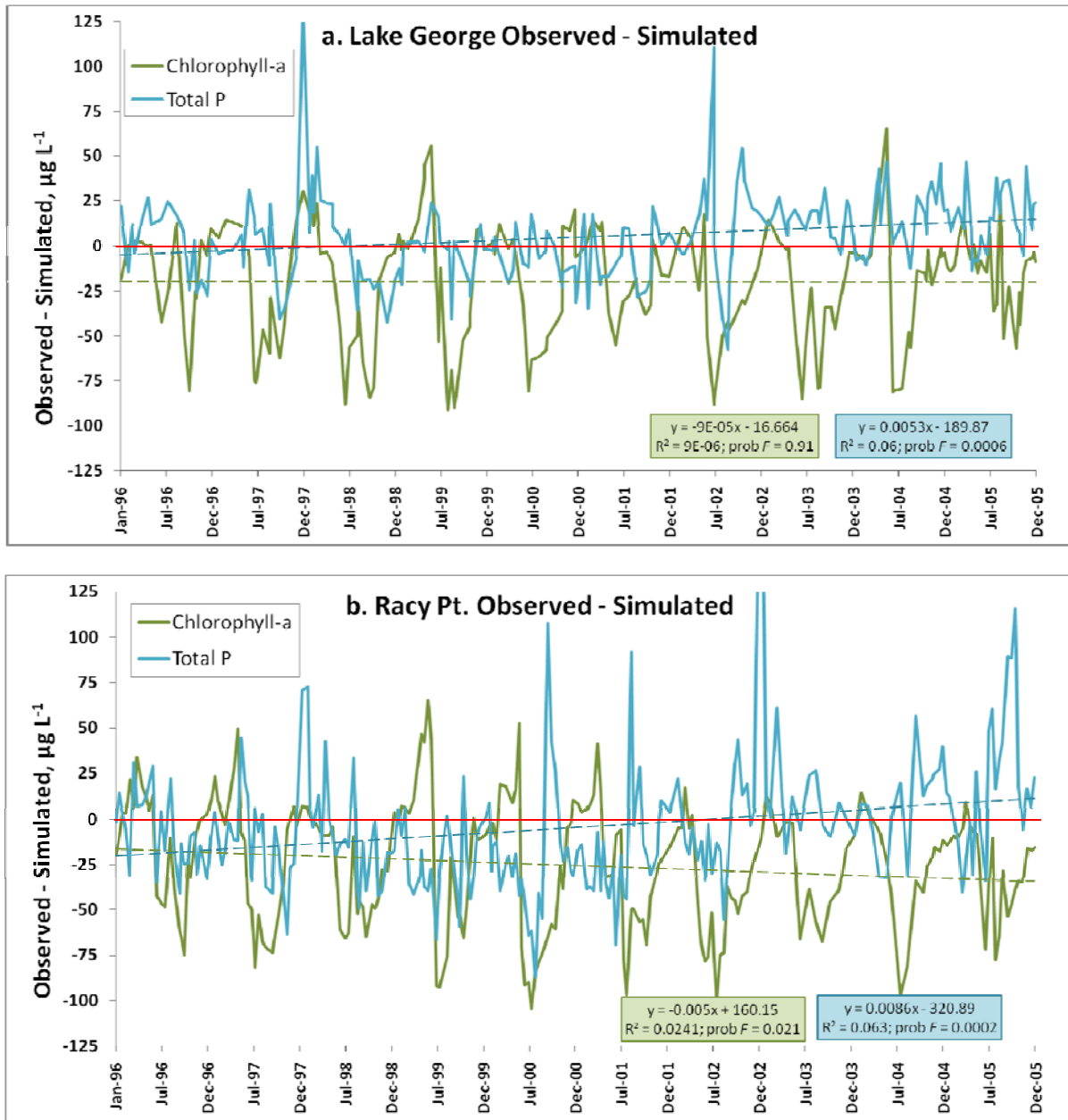


Figure 15. Time series of observed minus simulated chlorophyll-*a* (green) and TP (blue) at (a) Lake George and (b) Racy Pt. Red line indicates zero.

Table 4. Annual medians for differences between observed - simulated chlorophyll-*a* and total phosphorus concentrations for Lake George and Racy Pt. Asterisks indicate significance level of annual differences (observed – simulated) based on Wilcoxon signed ranks test for paired observations; * = 0.05; ** = 0.025; *** = 0.01; **** = 0.0005.

	Lake George		Racy Pt.	
	Chlorophyll- <i>a</i>	Total P	Chlorophyll- <i>a</i>	Total P
1996	-0.3	0.008	-10.5***	-0.007
1997	-13.4	-0.003	-6.3***	-0.010***
1998	-12.5***	0.006	-27.2****	-0.012
1999	-2.1	-0.002	-6.1	-0.023****
2000	-5.5**	-0.008**	-9.9****	-0.026***
2001	-17.3****	-0.010*	-26.2****	-0.020****
2002	-29.6****	0.016	-41.9****	-0.004
2003	-27.9****	0.014****	-15.8****	0.009
2004	-8.1***	0.013****	-20.7****	0.012
2005	-9.7****	0.015****	-16.4****	0.016**

While observed and simulated chlorophyll-*a* are significantly correlated, the tendency for the model to maintain elevated bloom biomass results in slopes of linear regressions relating simulated (independent) to observed (dependent) values significantly less than 1 (Figure 16a). The timing of simulated bloom rise in some instances leads to large discrepancies in simulated and observed values. For example, shifting the 1999 Racy Pt. simulated chlorophyll-*a* data series 25 days sooner increases the Pearson product-moment correlation from 0.37 to 0.60. Comparison of maximum chlorophyll-*a* (Figure 16b) indicates that at both Lake George and Racy Pt., the simulated values are greater than the observed for years when bloom peaks are less than 100 µg/L. Some of this discrepancy may arise from missed bloom peaks in the ambient monitoring data (which the model never misses as it predicts values for every day), though the preponderance of high simulated chlorophyll *a* maximums at the low end of the range suggests a systematic over-prediction by the model under some conditions.

As was demonstrated by the empirical models (Chapter 8. Plankton), discharge and residence time (expressed as water age or inverse water age) are correlated with bloom duration and maximum chlorophyll *a*. Theoretically, phytoplankton peak biomass should increase with increasing segment residence time, due to greater exploitation of growth resources and lower dilution from tributary inflow.

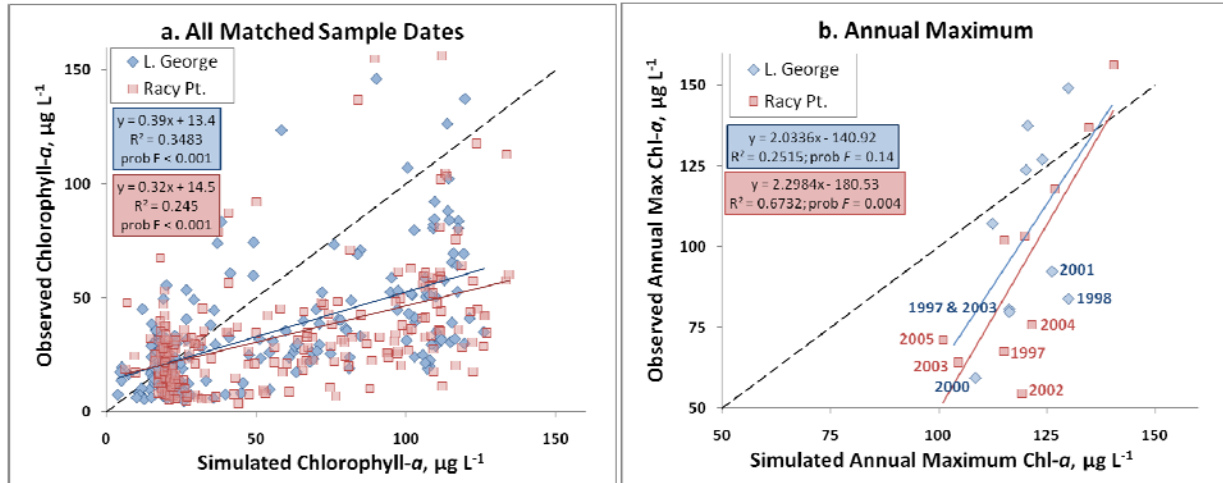


Figure 16. Comparison of (a) Same-date, and (b) Bloom season maximum simulated and observed chlorophyll-*a* for Lake George and Racy Pt. samples.

Due to the longer residence time and prevailing lower concentration, phosphorus is growth-limiting more often in Lake George than at Racy Point (peak bloom biomass is dominated by N-fixing cyanobacteria, hence N limits the rate of bloom expansion but not peak biomass), a tendency that has been confirmed in nutrient enrichment and dilution assays (Paerl et al. 2005). The result is that for Lake George, water age (a measure of residence time) or discharge alone is uncorrelated with bloom season maximum chlorophyll-*a* (Figure 17a and 18a). Conversely, higher prevailing phosphorus concentrations at Racy Pt. allow the phytoplankton to benefit from longer residence time or lower discharge, and these measures account for a larger amount of the variance in maximum chlorophyll-*a* (Figure 17b and 18b). Though a shift in the absolute magnitude of maximum chlorophyll *a* is apparent between the observed and simulated maximum values, the relative trends with respect to water age and discharge are the same: water age and discharge are uncorrelated with maximum chlorophyll *a* in Lake George, but are more strongly correlated at Racy Pt.

The more frequent condition of phosphorus limitation in Lake George leads to greater exploitation of the available supply as water age increases or discharge decreases. If the mean seasonal chlorophyll-*a*:TP ratio is used as a coarse index of phytoplankton competition for phosphorus, it can be seen that this ratio is strongly correlated with water age and discharge (Figure 17c and 18c) in both the observed and simulated data. The observed data chlorophyll-*a*:TP ratio is also significantly correlated with water age and discharge at Racy Pt. (Figure 17d and 18d), though with a lower R^2 value, as would be expected where phosphorus exerts a lower influence over maximum phytoplankton biomass. Simulated chlorophyll-*a*:TP ratio is poorly correlated with mean water age and discharge, presumably due to the higher loading of the simulated input data, resulting in little or no P limitation in modeled phytoplankton.

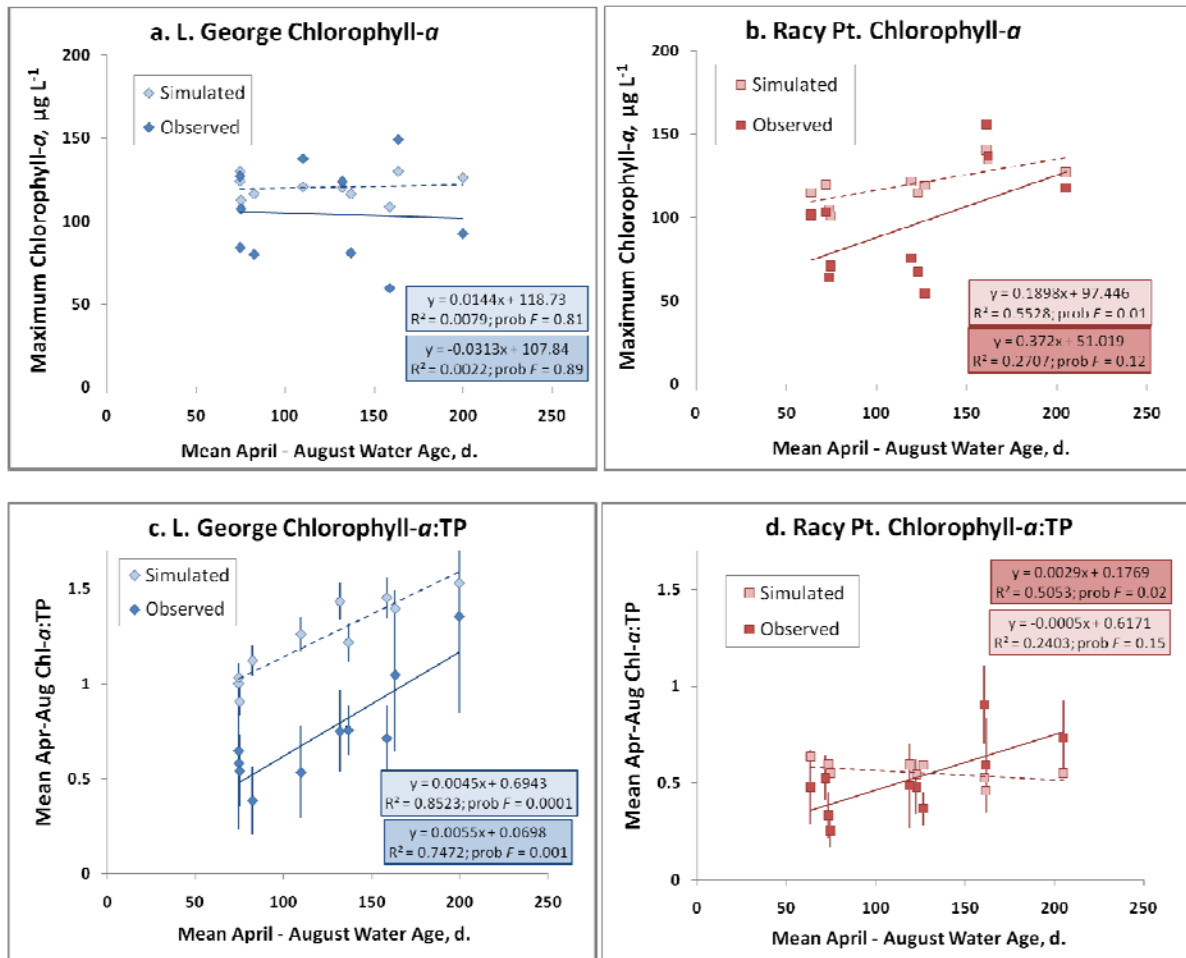


Figure 17. Relationships between annual mean bloom season water age and observed and simulated annual maximum chlorophyll-*a* (panels a and c) and chlorophyll-*a*:TP Ratio (panels b and d).

Water Withdrawal Scenario Simulations

Eight water withdrawal scenarios were simulated with CE-QUAL-ICM. Three are examined here: FwOR1995PN, FwOR2030PS, and FwOR1995NN (see Chapter 8. Plankton for a description of withdrawal scenarios). Though not considered a realistic scenario, statistics from the FwOR1995NN scenario are included as it represents the largest net reduction in discharge and concomitant increase in water age (Table 2). In some instances, statistics from the FULL1995PN and FULL2030PS scenarios are included, to aid in elucidating the effect at Racy Pt. of stepped levels of discharge reduction with the addition of the Ocklawaha River withdrawal. The range in water age increases for these scenarios, with respect to the BASE1995NN scenario, are listed in Table 5.

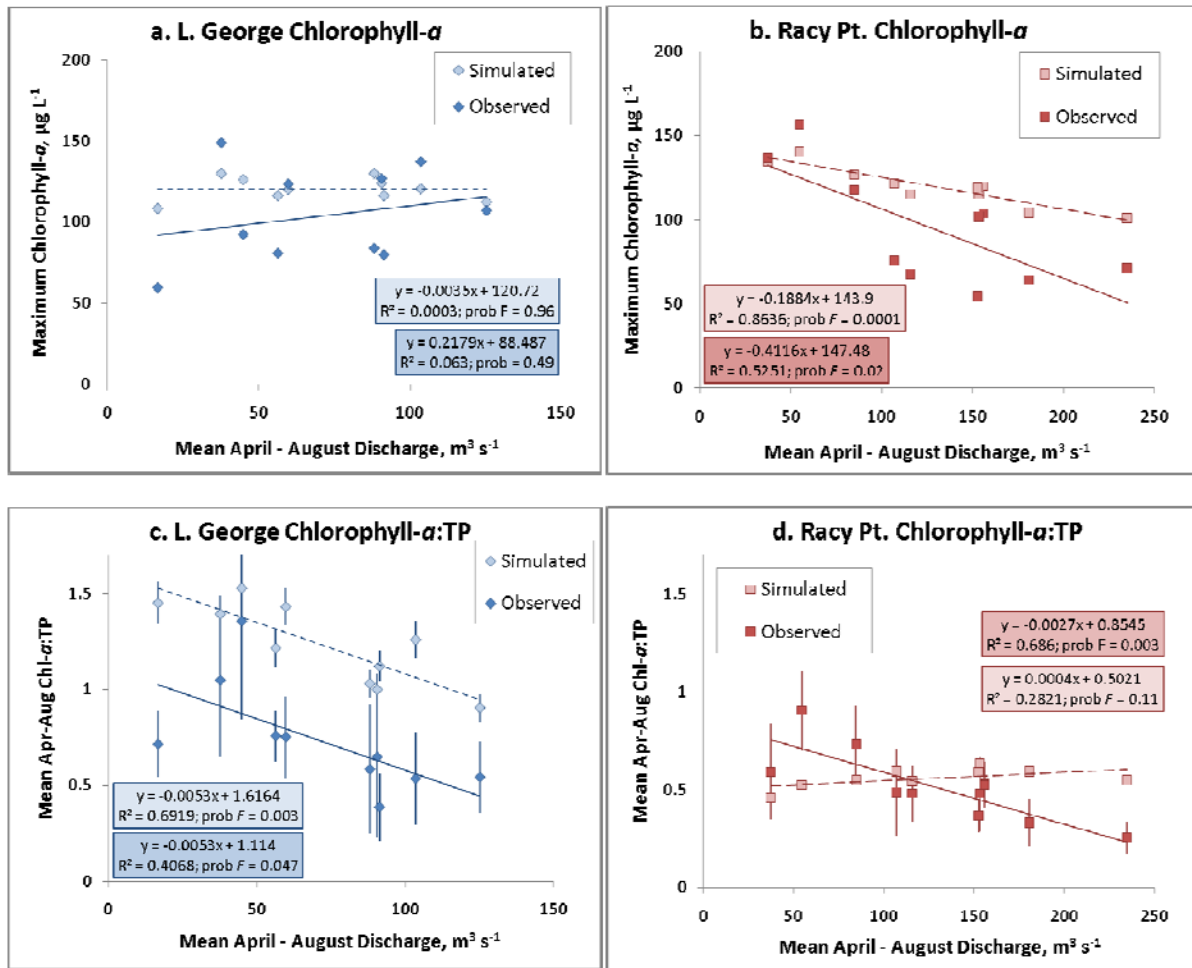


Figure 18. Relationships between mean bloom season discharge and observed and simulated annual maximum chlorophyll-*a* (panels a and c) and chlorophyll-*a*:TP ratio (panels b and d).

Table 5. Increases in mean April – August water age over the base case at Lake George and Racy Pt. for priority withdrawal scenarios. Base scenario is BASE1995NN.

Scenario	Lake George				Racy Point			
	Annual Minimum Increase		Annual Maximum Increase		Annual Minimum Increase		Annual Maximum Increase	
	Days	Year	Days	Year	Days	Year	Days	Year
FULL1995PN	1.7	2002	9.0	2001	0.7	2003	3.3	2001
FwOR1995PN	1.9	1998	10.5	2001	2.4	1998	13.6	2001
FULL2030PS	2.0	2002	8.7	2000	0.8	2001	3.7	2000
FwOR2030PS	2.0	2005	10.3	2000	3.5	2003	13.0	1999
FwOR1995NN	2.3	1998	12.6	2001	2.5	1998	14.3	2001

Changes from the base case in median annual maximum chlorophyll-*a* for withdrawal scenarios derived from the CE-QUAL simulations are listed in Table 6. Greatest percent increases in maximum chlorophyll-*a* are predicted to occur in Lake George, and the largest 10-year median

increase is 1.7 percent for the FWOR1995PN case. The small changes in median bloom maximum chlorophyll-*a* predicted by CE-QUAL-ICM under withdrawal scenarios (Table 6, Figure 19) support the results of empirical models that predicted similar, small changes (see Chapter 8. Plankton).

As was seen in the calibration comparison between the observed and simulated data, withdrawal scenario bloom season mean water age and maximum chlorophyll-*a* are poorly correlated, or uncorrelated, in Lake George, but are significantly correlated at Racy Pt. (Figure 19). The predicted differences in scenario maximum chlorophyll-*a* are small relative to inter-annual differences, a result that is not surprising, as scenario water age differences are small relative to the inter-annual differences.

Table 6. Withdrawal scenario percent change in 1996-2005 median maximum chlorophyll-*a* with respect to the base case BASE1995NN.

Scenario	Lake George	Racy Pt.
FULL1995PN	1.7 %	-0.4 %
FwOR1995PN	1.7%	0.0 %
FwOR2030PS	0.0 %	-0.1 %
FwOR2030NN	1.7 %	-0.1 %

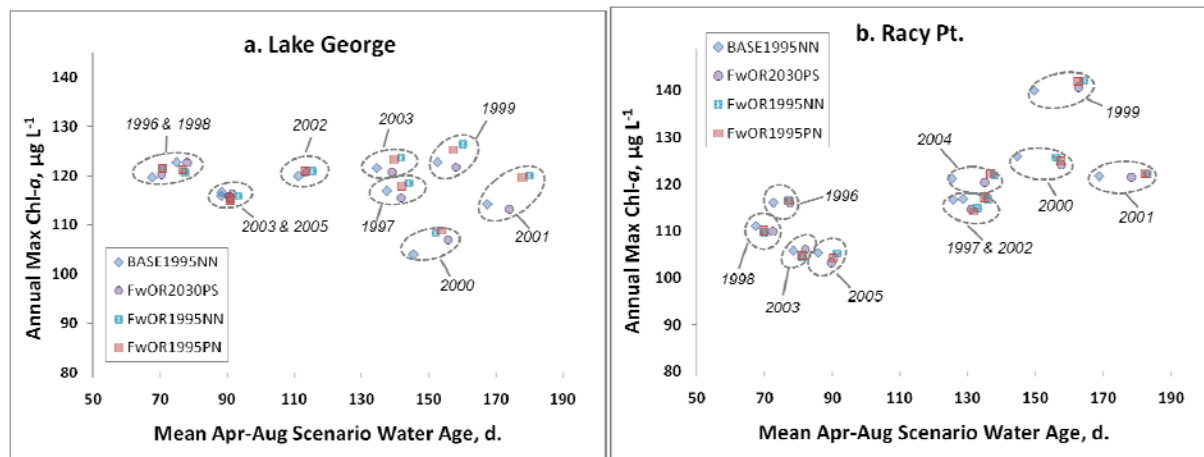


Figure 19. Relationship between water age and April – August maximum chlorophyll-*a* for CE-QUAL-ICM withdrawal scenario simulations.

The scatter plots of Figure 20a-d compare the percent change in predicted maximum chlorophyll-*a* to the water age increases over the BASE condition for the 10 simulation years from 1996 - 2005. The results of the FULL1995PN scenario are added here to help assess the partial effect of the proposed Ocklawaha withdrawal on the downstream Racy Pt. location. For

the FwOR1995PN and FwOR1995NN scenarios, water age increase and maximum chlorophyll-*a* percent change are significantly and positively correlated, with stronger correlation and larger percent increases exhibited for Lake George than for Racy Pt (Figure 20b,c). For three of the 10 simulated years at Lake George, and for more than half of the years at Racy Pt., predicted maximum chlorophyll-*a* is lower under the respective withdrawal scenario. Water age increases under the FULL1995PN scenario are relatively small at Racy Pt., and the resulting relationship between water age change and percent change in maximum chlorophyll-*a* is not significant (Figure 20a). Scenarios with an Ocklawaha River withdrawal appear to have sufficient range in water age difference to elucidate a positive relationship, though weak, between water age and maximum chlorophyll-*a* at Racy Pt. The greatest predicted increase in maximum chlorophyll-*a* is 5.4 percent in Lake George under the FwOR1995PN scenario, corresponding to a 10.5 day increase in water age in 2001. The largest percent increase at Racy Pt. is 1.6 percent, corresponding to a 14.8 day increase in mean water age in 1999 under the FwOR1995NN scenario.

For the FwOR2030PS scenario based on the 2030 land use and sea level rise, the significance of the relationships between maximum chlorophyll-*a* change and water age increase is much lower, or non-existent. Under these scenarios, despite some large increases in water age, annual maximum chlorophyll-*a* is, in most years, predicted to decrease from the base case (Figure 20d).

Factors Contributing to Scenario Outcomes

Salinity, color, and TP exert significant influence over cyanobacteria growth and maximum standing stock in the freshwater SJRE, and in the SJREM. These growth-relevant constituents exhibit longitudinal concentration changes due to the proportion of source water and changes in loads at various points in the SJRE. Proposed water withdrawals will change the relative proportions of these sources, altering the balance of these constituents and potentially changing cyanobacteria productivity. The expected direction of these changes can be construed from location, volume, and concentration characteristics of the inputs to the river, as shown in Figure 21.

St. Johns River water entering Lake George is high in dissolved solids, color, and TP. Within the lake, three large springs add constant baseflow that is clear, low in TP and high in dissolved solids. The confluence with the Ocklawaha downstream of Lake George adds a large volume of water that is relatively low in dissolved solids, color, and TP, and dilutes and lowers constituent concentrations below its confluence with the St. Johns.

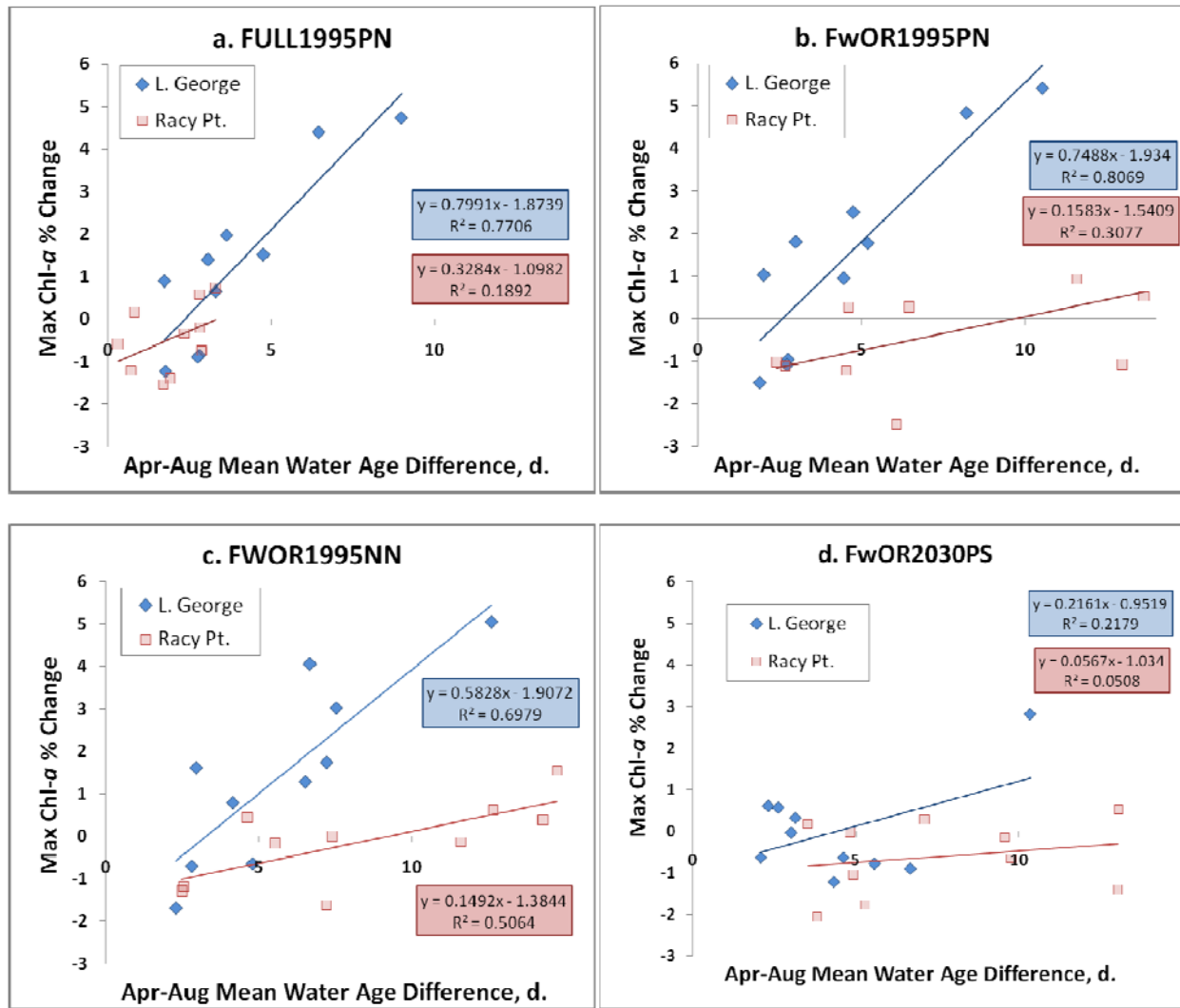
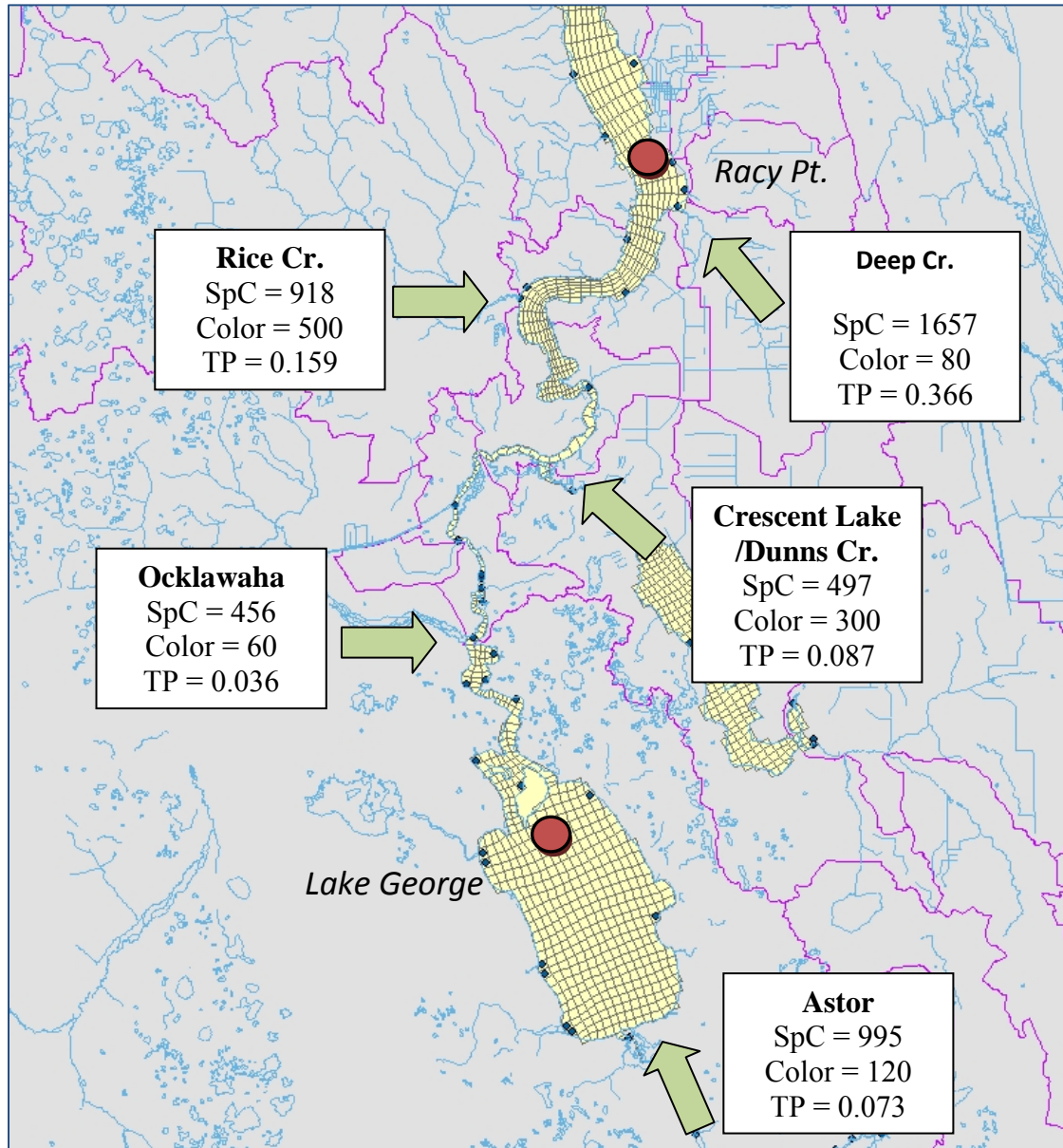


Figure 20. Comparison between April – August mean water age increase and percent change in maximum chlorophyll-a over the base case.

Dunns Creek, the next major tributary entering the SJRE, is relatively low in dissolved solids, but high in TP and color. Downstream of Dunns Creek, pulp mill effluent and agricultural runoff add color and TP, and can be a large proportional contributor of dissolved solids during low flow, when point source volume and irrigation runoff constitute a large portion of total segment inflow. Hence, in-river constituent concentration changes can arise from two different mechanisms in withdrawal scenario simulations: from re-concentration of the input loads from water withdrawal volume reduction in the middle St. Johns and Ocklawaha (discussed in the “Model Inputs” section), and from longitudinal change in the proportion of source water of different constituent character.

Figure 21. Major inputs to the freshwater SJRE, and the median concentrations of these inputs of specific conductance (SpC, $\mu\text{mho/cm}$), color (Pt-Co Units), and TP (mg/L).



To assess the level of concentration change and the potential contribution to cyanobacteria bloom magnitude, the bloom season (Apr. – Aug.) mean changes in salinity, color, and TP under the FwOR1995PN, FwOR2030PS, and FwOR1995NN scenarios for each simulation year were compiled, and are compared in Tables 6 – 8. Color is predicted from the model refractory dissolved organic carbon (RDOC) variable, as this variable is calibrated specifically in the external load to represent colored dissolved organic matter and affect underwater light attenuation. Color is predicted from RDOC by the following equation:

$$\text{Color, PCU} = (0.669 * \text{RDOC} + 2.537)^2 ,$$

where RDOC is measured in mg/L.

Both relative and absolute changes in salinity arising from water withdrawals are small (Table 6). The largest projected increase over the BASE salinity is 2.4 percent in 2000 under the FwOR2030PS scenario. In general, predicted relative increases are greater for Racy Pt. than for Lake George. Average Racy Pt. salinity increases are greater under the upper basin project scenarios, with the largest increases occurring under low-flow years (1999 – 2001). The maximum mean salinity encountered under any scenario is 0.84 psu in Lake George in 2001, below the level that would inhibit cyanobacteria growth.

Large relative changes are predicted under some scenarios for color and TP. Color increases as high as 31 percent over the BASE scenario mean are predicted for Racy Pt., from 118 to 155 Pt-Co units in 2000. Relative increases in color are larger for Racy Pt. than for Lake George, reflecting the proportionally greater volume of highly colored inputs downstream of water withdrawals. Relative increases in predicted scenario color values are variable for Lake George, and are not related to water age. This may be due to the influence of artesian spring flow contributions to the lake, which offset boundary re-concentration effects on overall lake color. Conversely, predicted color increases at Racy Pt. are strongly positively correlated with withdrawal scenario water age differences. Linear regressions relating increase in mean water age to percent change in color predict increases in color of over 20 percent for water age increases greater than 10 days under the FwOR1995NN and FwOR1995PN scenarios.

Table 6. Base scenario mean and maximum salinity, and the percent increase in salinity under withdrawal scenarios.

		FwOR1995PN	FwOR2030PS	FwOR1995NN
YEAR	BASE Apr-Aug Mean Salinity, psu	Mean Percent Change From BASE Scenario Salinity		
Lake George				
1996	0.52	0.6	0.2	0.5
1997	0.61	0.5	-0.4	0.7
1998	0.33	0.0	0.8	0.0
1999	0.73	0.2	0.2	0.2
2000	0.62	-0.1	-0.1	0.1
2001	0.82	1.3	-0.1	1.5
2002	0.61	-0.4	-1.7	-0.1
2003	0.43	0.7	1.0	0.7
2004	0.69	-0.2	-0.1	-0.4
2005	0.46	-0.3	-1.5	0.5
Racy Pt.				
1996	0.44	1.1	0.7	1.1
1997	0.45	0.8	0.8	0.5
1998	0.30	0.2	-0.6	0.2
1999	0.54	1.2	2.3	0.0
2000	0.44	0.6	2.4	0.0
2001	0.62	2.1	2.3	2.0
2002	0.48	-0.1	0.6	-0.3
2003	0.33	0.5	1.0	0.1
2004	0.51	1.4	1.6	1.0
2005	0.36	0.6	0.2	0.2

Table 7. Base scenario mean and maximum color, and the percent increase in color under withdrawal scenarios.

		FwOR1995PN	FwOR2030PS	FwOR1995NN
YEAR	BASE Apr- Aug Mean Color, PCU	Mean Percent Change From BASE Scenario		
Lake George				
1996	150	10.7	-0.7	10.6
1997	73	7.4	-1.2	12.1
1998	235	10.4	4.4	11.4
1999	66	9.8	0.8	14.7
2000	107	28.4	18.3	18.8
2001	50	12.6	0.4	13.7
2002	98	7.8	2.2	9.5
2003	161	9.9	2.1	10.6
2004	82	11.6	0.0	14.1
2005	142	10.1	1.2	9.9
Racy Pt.				
1996	193	11.8	2.5	11.4
1997	111	12.4	4.0	15.4
1998	211	9.1	7.3	9.0
1999	85	20.9	11.1	25.4
2000	118	31.1	20.8	23.9
2001	65	21.5	4.7	22.1
2002	111	13.6	7.6	11.7
2003	185	8.1	2.3	8.6
2004	108	20.2	6.5	22.7
2005	119	13.9	5.6	12.0

Table 8. Mean and maximum TP at Lake George and Racy Pt., and the percent increase in the mean and maximum under water withdrawal scenarios.

		FwOR1995PN	FwOR2030PS	FwOR1995NN
YEAR	BASE Apr- Aug Mean TP	Mean Percent Change From BASE Scenario		
Lake George				
1996	0.068	5.9	0.4	5.4
1997	0.059	4.3	-1.5	6.7
1998	0.076	5.3	2.8	5.9
1999	0.056	6.5	0.6	9.8
2000	0.050	11.9	6.5	8.6
2001	0.048	8.4	-0.4	9.1
2002	0.075	3.7	0.7	4.5
2003	0.074	4.6	1.1	5.1
2004	0.059	6.1	-0.1	7.5
2005	0.079	4.1	-0.7	4.8
Racy Pt.				
1996	0.097	6.9	2.5	6.7
1997	0.101	8.3	2.3	9.9
1998	0.091	5.2	6.0	5.4
1999	0.101	12.3	5.8	14.9
2000	0.094	15.0	8.3	14.8
2001	0.077	16.0	2.8	16.4
2002	0.100	7.7	4.1	7.1
2003	0.099	5.0	1.4	5.4
2004	0.094	12.5	4.2	13.7
2005	0.121	5.7	0.7	6.6

The highest April – August mean phosphorus concentration increases are 12 percent for Lake George in 2000 under the FwOR1995PN scenario, and 16 percent for Racy Pt. in 2001 under the FwOR1995NN scenario. As was the case for color, TP increases are predicted to be greater for Racy Pt. than for Lake George. Under the 1995 land use scenarios, both Lake George and Racy Pt. TP increases are strongly positively correlated with the increasing water age. For the 2030 land use, TP increase is correlated with water age increase for Racy Pt., but not for Lake George.

The potential positive and negative effects of increases in TP and color on bloom maximum chlorophyll-*a* might help explain these withdrawal scenario simulation results. In Lake George, due to the lower prevailing color level, and the inputs of clear water from artesian spring flow that are proportionally higher during low flow, color increases would theoretically pose a relatively small limitation on potential phytoplankton growth. The more frequent condition of phosphorus limitation in Lake George would however lead one to suspect that the strong relationship between greater water age and percent increase in maximum chlorophyll-*a* derives in part from increases in TP. Conversely, as phosphorus is more often in excess of phytoplankton growth needs at Racy Pt. (at least in the simulations), additions of phosphorus in these scenarios would not be expected to have a large effect on maximum chlorophyll-*a*, and predicted increases in color would be expected to exert a greater effect in counteracting phosphorus increase.

Another factor with potential implications for the achievement of maximum chlorophyll-*a* is increased water depth, which would occur under the FwOR2030PS scenario. Sea level rise associated with this scenario represents about a 5 percent increase in total depth, though may be a greater fraction of the phytoplankton mixed depth. This, in concert with increased color, may be enough to lower the ratio of photic zone to the total depth, reducing the vertical net primary production in the mixed water column. Sea level rise and segment volume increase also has the effect of increasing water age at equivalent discharge. Comparison of the difference between scenario and base mean 1996 – 2005 water age to the mean discharge reveals that under the FULL1995PN case, the mean percent decrease in Astor discharge of 6.5 percent is associated with a mean water age increase at Lake George of 3.4 percent. For this same scenario, the Palatka mean discharge decrease of 3.6 percent is matched by a 1.7 percent increase in Racy Pt. water age. Conversely, under the FULL2030PS case, Astor 1996 – 2005 discharge *increases* by 3.3 percent, and Lake George water age increases by 3.4 percent, while Palatka discharge increases by 4.8 percent, with Racy Pt. water age increasing by 1.9 percent. Under the FwOR2030PS case, Palatka mean discharge increases by 1.1 percent, while Racy Pt. mean water age increases by 6.5 percent (the Lake George water age – discharge relationship remains the same). Due to the difference in the discharge and water age relationship, effects of water withdrawals are intertwined with effects of sea level rise for future scenarios.

LITERATURE CITED

- Adamus, C. and M Bergman. 1993. Development of a Nonpoint Source Pollution Load Screening Model. Water Resources Department Technical Memorandum No. 1, St. Johns River Water Management District, Palatka , FL. 37 pp.
- Bratbak, G., J.K. Egge and M. Heldal. 1993. Viral mortality of the marine alga *Emiliana huxleyi* (Haptophyceae) and termination of algal blooms. Mar. Ecol. Prog. Ser. 93: 39-48.
- Brussaard, C.P.D., et al. 1995. Effects of grazing, sedimentation, and phytoplankton cell lysis on the structure of a coastal pelagic food web. Mar. Ecol. Prog. Ser. 123: 259-271.
- Cerco, C.F. and T. Cole. 1993. Three dimensional eutrophication model of Chesapeake Bay. J. of Environmental Eng. 119:1006-1025.
- Chalk, E.A., 1981. Cladoceran filter feeding in a Thames Valley reservoir. Ph.D. Thesis, CNAA. Central London Polytechnic and Thames Water Authority, 226 pp.
- Cloern, J.E., C. Grenz and L. Vidergar-Lucas. An empirical model of the phytoplankton chlorophyll:carbon ratio – The conversion factor between productivity and growth rate. Limnol. Oceanogr. 40(7): 1313-1321.
- DiToro, D.M. and J. J. Fitzpatrick. 1993. Chesapeake Bay Sediment Flux Model. USACE Contract Report EL-93-2. USACE Engineer Research and Development Center, Vicksburg, MS. 316 pp.
- Gallegos, C.L. 2005. Optical water quality of a blackwater river estuary: the Lower St. Johns River, Florida. Estuarine, Coastal and Shelf Science 63: 57-72.
- Geider, R.J. 1987. Light and temperature dependence of the carbon to chlorophyll-a ratio in microalgae and cyanobacteria: Implications for physiology and growth of phytoplankton. New Phytol. 106: 1-34.
- Gosselain, V., B.P. Hamilton and J-P. Descy. 2000. Estimating phytoplankton carbon from microscopic cell counts: An application to riverine systems. *Hydrobiologia* 438: 75-90.
- Hamrick, J. M. 1992. A Three-dimensional Environmental Fluid Dynamics Computer Code: Theoretical and Computational Aspects. Special Rept. 317. The College of William and Mary, Virginia Inst. of Marine Sciences, Virginia.
- Hendrickson, J., N. Trahan, E. Gordon and Y. Ouyang. 2007. Estimating the relevance of organic carbon, nitrogen, and phosphorus loads to a blackwater river estuary. J. American Water Resources Assoc. 43(1): 264-279.

- Hendrickson, J.C., and C. Hart. 2007. Determination of Nitrogen and Phosphorus Non-Point Source Loads for Urban Stormwater Jurisdictions of the Lower St. Johns River Basin. Technical Memo Provided to the LSJR TMDL Executive Committee for Allocation of the Nutrient Pollution Load.
- Hendrickson, J.C. and J. Konwinski. 1998. Seasonal Nutrient Import-Export Budgets for the Lower St. Johns River, Florida. Final Report, Contract No. WM598, Florida Department of Environmental Protection, Tallahassee, FL. 109 pp.
- Hessen, D.O., E. Van Donk and R. Gulati. 2005. Seasonal seston stoichiometry: effects on zooplankton in cyanobacteria-dominated lakes. *J. Plankton Res.* 27(5): 449-460.
- Jahnke, J. and D.M. Mahlmann. 2010. Differences in cellular dry weight per unit biovolume of *Phormidium autumnnale* (Cyanobacteria) dependent on growth conditions. *J. Appl. Phycol.* 22: 117-122.
- Klausmeier, C.A., E. Litchman and S.A. Levin. 2004. Phytoplankton growth and stoichiometry under multiple nutrient limitation. *Limnology and Oceanography* 49(4, part 2): 1463-1470.
- Limno-Tech, Inc. 2005. Studies in Support of Sediment and Eutrophication Modeling in the Lower St. Johns River, Florida. Final Report, Contract SD174AA, St. Johns River Water Management District, Palatka, FL.
- Menden-Dauer, S. and E.J. Lessard. 2000. Carbon to volume relationships for dinflagellates, diatoms and other protist plankton. *Limnol. Oceanogr.* 45(3): 569-579.
- Moal, J., V. Martin-Jezequel, R.P. Harris, J-F Samain and S.A. Poulet. 1987. Interspecific and intraspecific variability of the chemical composition of marine phytoplankton. *Oceanol. Acta* 10: 339-346.
- Montagnes, D.J.S., J.A. Berges, P.J. Harrison and F.J.R. Taylor. 1994. Estimating carbon, nitrogen, protein and chlorophyll a from volume in marine phytoplankton. *Limnol. Oceanogr.* 39(5): 1044-1060.
- Mullin, M.M., P.R. Sloan and R.W. Epply. 1966. Relationship between carbon content, cell volume and area in phytoplankton. *Limnol. Oceanogr.* 11: 307-311.
- Paerl, H.W., J.J. Joyner, M. F. Piehler. 2005. Relationships Between Nutrient Conditions and Phytoplankton Community Structure and Function in the Lower St. Johns River. Final Report, Contract 99B170, St. Johns River Water Management District.
- Pollman, C.D. and S. Roy. 2003. Examination of Atmospheric Deposition Chemistry and its Effect on the Lower St. Johns Estuary. Tetra Tech. Gainesville, FL.

- Riemann, B., P. Simonsen, and L. Stensgaard. 1989. Carbon and chlorophyll content of phytoplankton from various nutrient regimes. *J. Plankton Res.* 11(5): 1037-1045.
- Redfield, A.C. 1958. The biological control of chemical factors in the environment. *American Scientist*.
- Reynolds, C.S. 1984. *The Ecology of Freshwater Phytoplankton*. Cambridge University Press.
- Rocha, O. and A. Duncan. 1985. The relationship between cell carbon and cell volume in freshwater algal species used in zooplanktonic studies. *J. Plankton Res.* 7: 279-294.
- Strathmann, R.R. 1967. Estimating the organic carbon content of phytoplankton from cell volume, cell area or plasma volume. *Limnol. Oceanogr.* 12: 411-418.
- Sucsy, P and J.C. Hendrickson. 2003. Calculation of Nutrient Reduction Goals for the Lower St. Johns River by application of CE-QUAL-ICM, a Mechanistic Water Quality Model. Department of Water Resources Draft Technical Memorandum, St. Johns River Water Management District, Palatka, FL. 91 pp.
- Tillman, D.H., C.F. Cerco, M.R. Noel, J.L. Martin and J. Hamrick. 2004. Three-Dimensional Eutrophication Model of the Lower St. Johns River, Florida. U.S. Army Corps of Engineers Engineer Research and Development Center Environmental Laboratory Report #ERDC/EL TR-04-13.
- Weinbauer, M.G., U. Christaki, J. Nedoma and K. Simek. 2003. Comparing the effects of resource enrichment and grazing on viral production in a meso-eutrophic reservoir. *Aquatic Microbial Ecol.* 31: 137-144.
- Williamson, S.J. and J.H. Paul. 2004. Nutrient stimulation of lytic phage production in bacterial populations of the Gulf of Mexico. *Aquatic Microbial Ecol.* 36: 9-17.
- Wilson, W.H., S. Turner and N.H. Mann. 1998. Population dynamics of phytoplankton and viruses in a phosphate-limited mesocosm and their effect on DMSP and DMS production. *Estuarine, Coastal and Shelf Sci.* 46(Supp. A): 49-59.
- Wilson, W.H., N.G. Carr and N.H. Mann. 1996. The effect of phosphate status on the kinetics of cyanophage infection in the oceanic cyanobacterium *Synechococcus* sp. WH7803. *J. Phycol.* 32: 506-516.